

Representative Sampling for Energetic Compounds at an Antitank Firing Range

Thomas F. Jenkins, Thomas A. Ranney, Alan D. Hewitt,
Marianne E. Walsh, and Kevin L. Bjella

April 2004

ERDC/CRREL TR-04-7

April 2004

Representative Sampling for Energetic Compounds at an Antitank Firing Range

Thomas F. Jenkins, Thomas A. Ranney, Alan D. Hewitt,
Marianne E. Walsh, and Kevin L. Bjella

Approved for public release; distribution is unlimited.

Prepared for U.S. ARMY CORPS OF ENGINEERS

ABSTRACT

Field sampling experiments were conducted at the CFB-Valcartier Arnhem antitank rocket range to investigate various sampling schemes that would yield representative soil samples at firing points and impact areas of antitank ranges. Three sampling strategies were evaluated. Between the firing point and the target, 10-m \times 10-m grids were established and 30-increment composite soil samples were collected. In two of these grids, one near the firing point and one at the target, the grids were divided into 100 1-m \times 1-m minigrids. Within each minigrid a discrete and a 10-increment composite soil sample were collected and analyzed for energetic compounds. In the target area, an alternative strategy was also evaluated using concentric halos around the target. Each halo was subdivided into increasing numbers of segments at increasing distances from the targets. Multi-increment composite samples were collected within each halo segment. Behind the firing line, nine line (linear) composites were collected at various distances from 0 to 25 m from the firing line. Results from the 100 1-m \times 1-m minigrids near the firing line and the target demonstrated that the distribution of analyte concentrations in the discrete samples was non-Gaussian and the range of concentrations varied over two orders of magnitude. The distributions of data for multi-increment composite samples with various numbers of increments were simulated by averaging the concentration estimates from randomly selected discrete samples. For the firing line area, the distribution of NG computed composites exhibits increased normality as the number of increments is increased and the resulting tolerance range declined substantially. This was also true for HMX in the target area. Recommendations are made for appropriate sampling strategies to collect representative surface soil samples for antitank rocket ranges.

DISCLAIMER: The contents of this report are not to be used for advertising, publication, or promotional purposes. Citation of trade names does not constitute an official endorsement or approval of the use of such commercial products. All product names and trademarks cited are the property of their respective owners. The findings of this report are not to be construed as an official Department of the Army position unless so designated by other authorized documents.
DESTROY THIS REPORT WHEN IT IS NO LONGER NEEDED. DO NOT RETURN TO THE ORIGINATOR.

CONTENTS

Preface	vi
1 Introduction	1
Representative Sampling	3
2 Objectives	6
3 Soil Sample Collection and Analysis	7
Soil Sample Collection	7
Water Sample Collection	10
Soil Sample Analysis	10
Water Sample Analysis	14
4 Results	15
Grid Samples from the Firing Point Past the Central Target	15
NG Concentrations Behind the Firing Line	17
Grid 3 Results for Discrete Samples from 100 1-m × 1-m Minigrids	17
Grid 10 Results for Discrete Samples from 100 1-m × 1-m Minigrids	27
Comparison of Discrete and 10-Increment Composite Samples for Grids 3 and 10	38
Results from Halo Sampling Pattern Around Central Target	38
Water Sample Results	48
Assessment of Subsampling Error for Composite Soil Samples	49
5 Summary and Recommendations	53
Major Residues and Locations on Antitank Rocket Ranges	53
Sampling Strategy for Characterization at Antitank Rocket Ranges	53
Soil Subsampling	54
Chemical Analysis of Soil Extracts	55
References	56

ILLUSTRATIONS

Figure 1. M72 Light Anti-Armor Weapon, also known as the LAW rocket	2
Figure 2. Concentric ring sampling pattern around targets	4

Figure 3. Antitank rocket range at CFB-Valcartier, Quebec	7
Figure 4. Twelve 10-m × 10-m grids located in a direct line from firing point number 2 to and beyond the center target	8
Figure 5. Grids 3 and 10 subdivided into 100 1-m × 1-m minigrids	9
Figure 6. Concentration of NG in composite soil samples collected in front of and behind the rocket firing line	11
Figure 7. Intermittent stream at edge of antitank range	12
Figure 8. Discrete and composite soil sampling in Grid 3	18
Figure 9. Distribution of NG concentrations for the 100 discrete soil samples collected in Grid 3	22
Figure 10. NG concentrations in 100 discrete soil samples collected in Grid 3	23
Figure 11. Distribution of the log NG concentrations for 100 discrete soil samples collected in Grid 3	23
Figure 12. NG concentrations for 100 discrete soil samples from Grid 3	24
Figure 13. NG concentrations found in discrete samples as a function of position within Grid 3	24
Figure 14. Plot of mean NG concentrations within each row relative to the firing point and target position	25
Figure 15. Distribution of NG concentration from mathematically generated composites of five increments	26
Figure 16. Distribution of NG concentration from mathematically generated composites of ten increments	28
Figure 17. Distribution of NG concentration from mathematically generated composites of 20 increments	28
Figure 18. Distribution of NG concentration from mathematically generated composites of 30 increments	29
Figure 19. Distribution of NG concentration from mathematically generated composites of 50 increments	29
Figure 20. Distribution of NG concentration from mathematically generated composites of 5 and 30 increments	30
Figure 21. Collecting discrete and composite soil samples in Grid 10	30
Figure 22. Distribution of HMX concentrations found in 100 discrete soil samples collected in Grid 10	34
Figure 23. Plot of HMX concentrations as a function of position within Grid 10	35
Figure 24. Plot of mean HMX concentrations within each row relative to the firing point and target position	35
Figure 25. Distribution of HMX concentrations from mathematically generated composites of five increments	37

Figure 26. Distribution of HMX concentrations from mathematically generated composites of 30 increments	37
Figure 27. Comparison of NG concentration in discrete and composite soil samples collected in Grid 3	45
Figure 28. Comparison of NG concentration in discrete and composite soil samples collected in Grid 3, minus the five pairs of data with the greatest differences	45
Figure 29. Comparison of HMX concentration in discrete and composite soil samples collected in Grid 10	46
Figure 30. Concentration of HMX relative to sample position around target ...	48
Figure 31. Concentration of NG relative to sample position around targets	49

TABLES

Table 1. Estimates of explosives detection limit for soil and water extraction..	13
Table 2. Analytical results for soil samples collected from Grids G2 through G12 and depth samples from Grids G2 and G10	16
Table 3. NG concentrations in soil behind anti-tank rocket firing point	17
Table 4. Analytical results from RP-HPLC analysis of discrete soil samples from 1-m × 1-m minigrids within Grid G3 near the firing line of antitank rockets	19
Table 5. Soil NG concentrations from mathematical composites of varying number of increments	27
Table 6. Analytical results from RP-HPLC analysis of discrete soil samples from 1-m × 1-m minigrids within Grid G10 near a target at the antitank range	31
Table 7. Soil HMX concentrations from mathematical composites of varying number of increments	36
Table 8. Soil concentrations, Grid 3	39
Table 9. Soil concentrations, Grid 10	42
Table 10. Analytical results from RP-HPLC analysis of composite soil samples collected in halo sections around target at various distances	47
Table 11. Analytical results for replicate subsamples of selected composite samples	50
Table 12. Mean % Relative standard deviation for laboratory duplicates	52

PREFACE

This report was prepared by Dr. Thomas F. Jenkins, Research Chemist; Alan D. Hewitt, Research Physical Scientist; Marianne E. Walsh, Chemical Engineer; and Kevin L. Bjella, Physical Science Technician, Environmental Sciences Branch, U.S. Army Engineer Research and Development Center (ERDC), Cold Regions Research and Engineering Laboratory (CRREL), Hanover, New Hampshire; and by Thomas A. Ranney, Science and Technology Corporation, Hanover, New Hampshire.

This research was funded by U.S. Army Corps of Engineers program “Characterization, Evaluation, and Remediation of Distributed Source Compounds (UXO-C) on Army Ranges.” The Technical Director and Program Manager for this work is Dr. John M. Cullinane and the Project Monitor is Dr. June Mirecki, both from the U.S. Army Engineer Research and Development Center, Environmental Laboratory, Vicksburg, Mississippi.

The authors thank Melanie Bouchard, Annie Gagnon, Andre Marois, Dominic Faucher, and Jeff Lewis of Defence Research and Development Canada–Valcartier (DRDC–Valcartier) for assistance in sampling the Arnhem antitank rocket range at Canadian Force Base Valcartier. Raynald Tremblay is acknowledged for providing EOD support during this sampling effort. The authors especially thank Dr. Sonia Thiboutot (DRDC–Valcartier) for arranging for our study at the Valcartier site and providing the data for the samples behind the firing line at the antitank firing range. Defence R&D Canada–Valcartier and Department of National Defence–Canada are acknowledged for allowing access to the Valcartier Arnhem range for conducting this study.

This report was reviewed by Dr. C.L. Grant, Professor Emeritus, University of New Hampshire, and Charles Ramsey, EnviroStat, Inc., Fort Collins, Colorado. The authors acknowledge the excellent suggestions made by both reviewers.

The Commander of the Engineer Research and Development Center is Colonel James R. Rowan, EN. The Director is Dr. James R. Houston.

Representative Sampling for Energetic Compounds at an Antitank Firing Range

THOMAS F. JENKINS, THOMAS A. RANNEY, ALAN D. HEWITT,
MARIANNE E. WALSH, AND KEVIN L. BJELLA

1 INTRODUCTION

Over the past several years, explosives residue characterization experiments have been conducted at a variety of military training ranges in the United States and Canada. These studies have included experiments at hand grenade ranges, antitank rocket ranges, artillery and mortar ranges, and tank firing ranges (sometimes called battleruns). This work was sponsored by the Strategic Environmental Research and Development Program (SERDP), the Director Land Forces Services (Canada), U.S. Army Alaska (USARAK), the U.S. Army Corps of Engineers, and the U.S. Army Environmental Center (AEC). These studies have vastly improved our understanding of the nature and extent of energetic compound contamination at Army training range impact areas and firing points.

Several studies have been conducted at antitank rocket ranges. The first of these was conducted at Canadian Force Base Valcartier (CFB-Valcartier), Quebec, in 1996 (Jenkins et al. 1997, Thiboutot et al. 1998). Additional studies have been conducted at a closed range at Fort Ord, California (Jenkins et al. 1998), and at three active live-fire ranges at Yakima Training Center, Washington (Pennington et al. 2002), CFB-Gagetown (Thiboutot et al. 2003), and at Fort Bliss's Doña Ana Range in New Mexico (Pennington et al. 2003).

The munition fired at each of these ranges is the 66-mm M72 Light Anti-Armor Weapon, sometimes referred to as the LAW Rocket (Fig. 1). This weapon has a warhead containing octol (70% HMX and 30% TNT) as the main charge, with a booster containing RDX. The double-based propellant used for this rocket contains 70% nitrocellulose (NC) and 30% nitroglycerin (NG).

Initial studies at antitank rocket ranges were concentrated on the impact areas near targets. The results indicated that HMX was present in surface soils at concentrations as high as several thousand mg/kg (ppm) adjacent to the targets, with

concentrations declining with distance from the targets (Jenkins et al. 1997, 1998; Thiboutot et al. 1998). Even though TNT was 30% of the main charge, the TNT concentrations in the surface soils were only about 1/100 of HMX. Samples collected from the shallow subsurface at Fort Ord indicated that the source zones for HMX and TNT at this range were at the surface in the top 15 cm (6 in.) of soil. Analysis of subsurface samples from Yakima Training Center showed that HMX concentrations decline about an order of magnitude at a 10-cm depth compared with the surface (Pennington et al. 2002). At Gagetown there appeared to be greater movement of HMX and TNT to the 10-cm depth than at Yakima, but only one core sample was analyzed (Thiboutot et al. 2003).

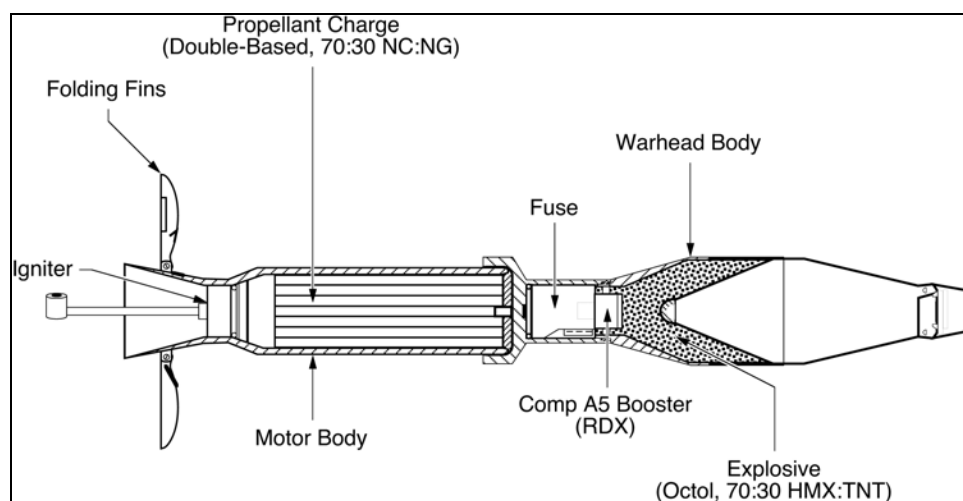


Figure 1. M72 Light Anti-Armor Weapon, also known as the LAW rocket.

The relatively high concentrations of HMX in surface soils at impact areas of antitank rocket ranges is thought to be due to the high incidence of duds with the M72 rockets. Some of these duds shear open upon impact, ejecting undetonated main charge chemicals. The HMX concentration in surface soil next to a ruptured LAW rocket at Yakima was 10,400 mg/kg (Pennington et al. 2002).

In the more recent studies at antitank rocket ranges, soil samples have been collected at firing points as well. At Yakima, only two samples were collected 5–10 m in front of the firing line and NG was detected at 1.8 and 3.6 mg/kg (Pennington et al. 2002). At Gagetown, samples were collected at distances 10, 20, and 50 m in front of the firing line and 2 and 5 m behind the firing line. In front of the firing line the NG concentrations in the surface soil samples ranged from 424 mg/kg at 10 m to 14.1 mg/kg at 50 m. The concentrations behind the firing line were even higher, with the highest value of 11,300 mg/kg (1.13%). At

Fort Bliss, NG was found at much lower concentrations in surface soils than at CFB–Gagetown, but it was detectable 20 m in front of the firing line and 10 m behind the firing line.

Representative Sampling

The largest source of uncertainty in the characterization of chemical contamination at sites contaminated with residues of energetic compounds is generally sampling error (Jenkins et al. 1996, 1997; Thiboutot et al. 1998). The major factor that causes this problem is distributional heterogeneity. For military training ranges the deposition of residues is often as particles of propellant near firing points and explosives at impact areas (Hewitt and Walsh 2003, Pennington et al. 2003).

A number of studies have been conducted in an attempt to understand the nature of the spatial heterogeneity in energetics distribution at training ranges, and to devise sampling strategies to enable the collection of representative soil samples to assess the degree of contamination. The short-range spatial heterogeneity was determined to be very large at antitank ranges, showing the futility of trying to use a small number of discrete soil samples to adequately represent the concentrations of explosives near targets (Jenkins et al. 1997, 1999). Based on these studies, a recommendation was made to use composite samples with replication in a concentric ring sampling pattern around targets (Fig. 2) to estimate mean concentrations within defined zones (Jenkins et al. 1998).

A study was conducted at Fort Greely, Alaska, to determine whether residues of energetic compounds were present at a testing range used by the Cold Regions Test Center. A number of sampling strategies were employed, including radial composites around artillery and mortar targets, line composites along a berm used for 40-mm grenade impacts, and line composites at a 40-mm firing point (Walsh et al. 2001). A recommendation from this work was that if the goal of sampling was to estimate the mean concentration for an area, a multi-increment composite sampling strategy should be employed. Walsh et al. (2001) recommended dividing the area into square grids with collection of duplicate multi-increment composite samples in each grid. Superimposed on these square grids are radial bands around targets where higher concentrations are expected.

Ampleman et al. (2003a, b) conducted a range assessment for residues of energetic compounds at CFB-Shilo in 2000 and 2001. They sampled both tank firing ranges and a hand grenade range in this study. At the target areas for the tank firing ranges they used circular multi-increment composite sampling with at least 20 increments per composite. In other areas of the tank range, they used line composites composed of at least 20 increments at various distances between the

firing point and target of tank firing ranges. At the grenade range, they collected line composite samples. Ampleman et al. concluded that the residues of explosives at the hand grenade range were much more uniform than at other types of training ranges due to the large numbers of explosions that mixed the soil.

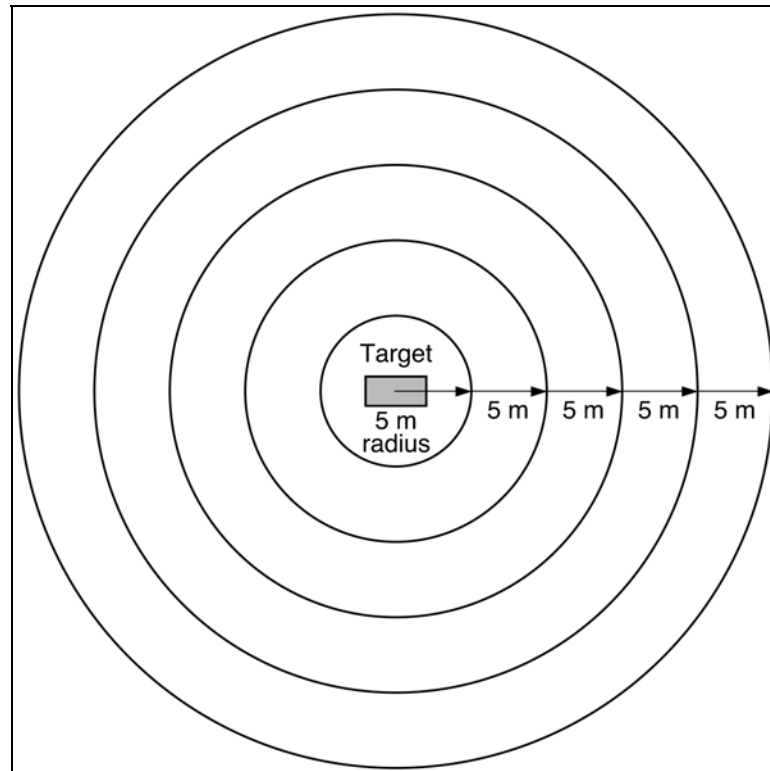


Figure 2. Concentric ring sampling pattern around targets.

Walsh* conducted a study at a hand grenade range at Fort Wainwright, Alaska, in which a 10-m \times 10-m area was marked off and a series of multi-increment composite samples was collected. The number of increments (n) per composite was varied (5, 10, 20, 40) and five replicates for each value of n were collected. The results indicated that the mean value for the different values of n was not significantly different, but the variance was reduced substantially as the value of n increased.

The distribution of residues of explosives at training ranges is due to the manner in which contamination occurs. Thus, for different ranges and for different portions of the same range, the distributions may be quite different. For

* Personal communication, M.E. Walsh, ERDC-CRREL, 2001.

example, at the firing point area, the contamination is due to propellant residues deposited from the firing activity. For a howitzer, the propellant is consumed at firing, but for rockets, the propellant is consumed from the firing point to the target. Thus the area of deposition is likely quite different for residues from the firing of a howitzer and a shoulder-fired rocket system such as the M72 LAW rocket.

At the impact areas, residues can be deposited from high-order detonations, low-order (partial) detonations, or rupture of undetonated munitions. The degree to which a given type of munition undergoes these various fates is undoubtedly different for different munitions. For thin-walled LAW rockets, for example, the dud rate is high and the likelihood of rupture much greater for this munition than for a thick-walled artillery shell. For these reasons the sampling strategy for the collection of representative samples may need to be different for different ranges.

2 OBJECTIVES

The main objective of this study was to optimize the use of the multi-increment composite sampling approach for the collection of representative soil samples for characterization of the mean concentration of energetic compounds at specific areas of antitank rocket ranges. Because the mode of contamination and the major contaminants differ for the firing point area and the impact area, it was recognized that the sampling strategies for the two areas might need to be different, and several approaches were investigated. If possible, we hoped to provide data to allow choices to be made based on the level of uncertainty that was acceptable for a given investigation. One specific goal was to investigate the characterization uncertainty as a function of the number of increments in surface multi-increment composite soil samples. Another objective was to determine whether there was a concentration gradient in residues from propellants behind the firing line used for antitank rockets, and determine the distance behind the firing line where deposition occurs during the firing activity.

3 SOIL SAMPLE COLLECTION AND ANALYSIS

Soil Sample Collection

This study was conducted at the antitank rocket range at CFB-Valcartier, Quebec (Fig. 3) on 12 and 13 May 2003. This is an active range where shoulder-fired 66-mm M72 rockets (Fig. 1) are fired at targets located at least 110 meters from the firing point. Three armored personnel carrier targets are located on a flat area with two additional targets on the hillside above. This study was conducted in the level area between the firing point and the three targets, the closest of which was 110 meters from the firing point.



Figure 3. Antitank rocket range at CFB-Valcartier, Quebec.

A series of twelve 10-m \times 10-m grids were located in a direct line from firing point number 2 (the position thought to be the most used) to and beyond the center target (Fig. 4). The target was located within Grid 11, with Grid 12 located behind the target. Thirty-increment composite samples were collected using the random walk method from the surface to a 2.5-cm depth in Grids 2 through 12 using small stainless steel hand shovels. The hand shovels were wiped off and rinsed with acetone between sampling grids.

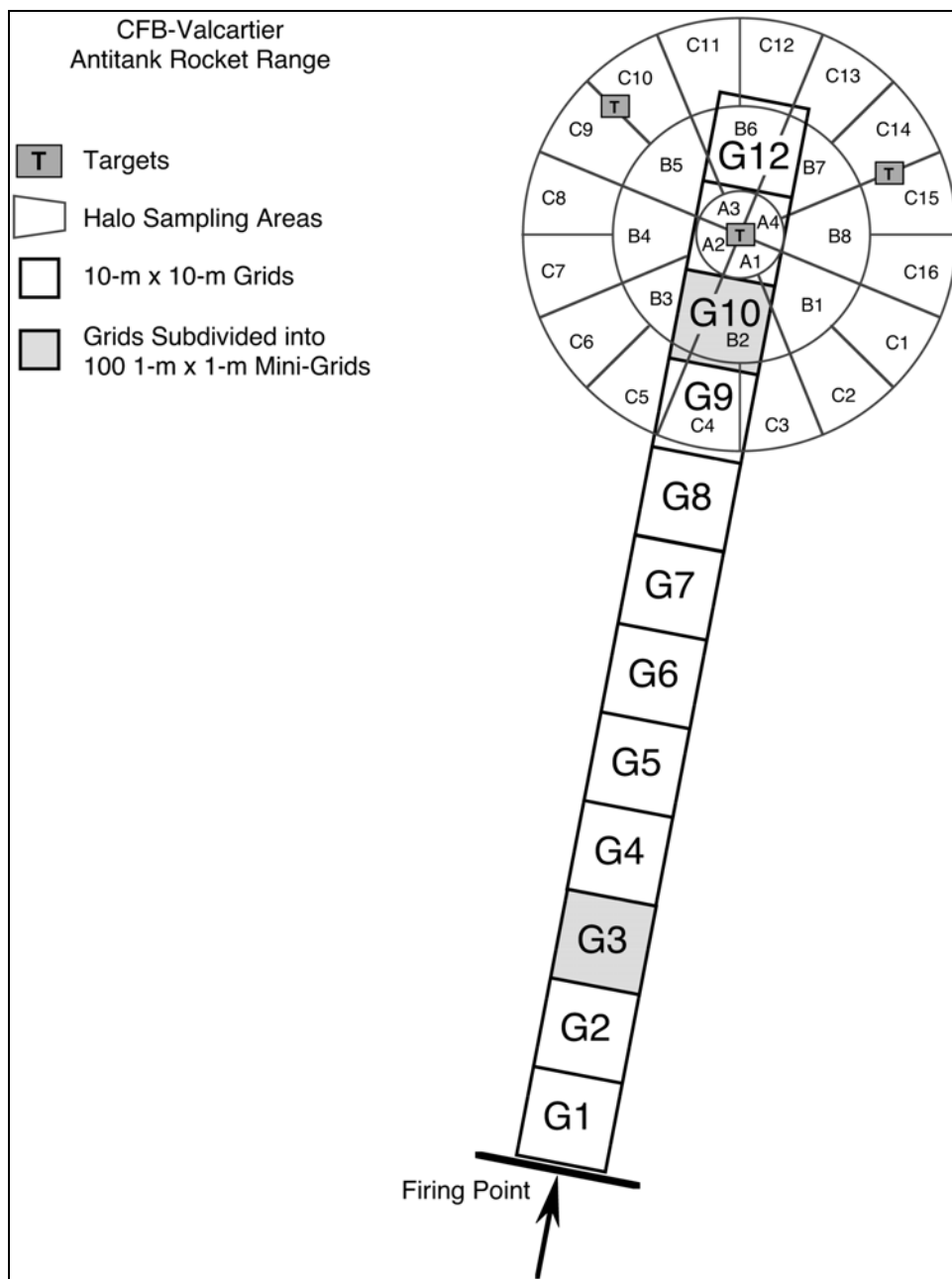


Figure 4. Twelve 10-m x 10-m grids located in a direct line from firing point number 2 to and beyond the center target and halo sampling areas around target.

After the 30-increment composite samples were collected, Grids 3 and 10 were each subdivided into 100 1-m x 1-m minigrids (Fig. 5). A discrete sample

and a 10-increment composite sample were collected at random positions within each minigrid using stainless steel hand shovels. An attempt was made to sample areas that did not have footprints from the collection of the 30-increment composite samples. For Grid 3, the depth sampled was 0 to 2.5 cm; for Grid 10 it was 0 to 1.5 cm. Discrete samples were placed in 4-oz. amber glass containers. Composite samples were placed in 18-in. × 30-in. clean polyethylene bags and closed with cable ties. Chunks of orangish-red-colored propellant were observed at the surface and in the shallow subsurface in Grid 10. These chunks gave a strong positive response to the spray from the second can of the EXPRAY Kit (Plexus Scientific, Silver Spring, Maryland), suggesting the presence of a nitramine or nitrate ester, probably nitroglycerin (NG). Shallow subsurface soil samples were also collected at two locations. The first was in Grid 2, near the boundary with Grid 1. The second was in Grid 10, near the boundary of Grid 11, just in front of the target. In each case, samples were collected at the following depths below ground surface: 0–2.5 cm, 2.5–5.0 cm, and 5.0–10 cm.



Figure 5. Grids 3 and 10 subdivided into 100 1-m × 1-m minigrids.

Another sampling strategy was employed in the area around the central target (Fig. 4). Three concentric rings were identified at distances of 5 m, 15 m, and 25 m from the target. These rings established sampling halos that were from the outside of the target to 5 m from the center of the target, from 5 m to 15 m from the center of the target, and from 15 m to 25 m from the target. The inside halo (halo A) was subdivided into four equal segments along the cardinal lines. Halos

B and C were subdivided into 8 and 16 segments, respectively, as shown in Figure 4. Within all 28 halo segments, 30-increment composite samples were collected randomly from the 0- to 2.5-cm depth using the random walk method and stored in clean polyethylene bags.

Two sets of linear, 10-increment line composite surface soil samples were also collected behind the firing line at distances of 0 m, 2.5 m, 5 m, 7.5 m, 10 m, 12.5, 15 m, 20 m, and 25 m (Fig. 6). The segments sampled for each set were 11.5 m in length. Individual increments for these two sets of line composites were collected systematically across these 11.5-m segments. These samples were collected by our Canadian colleagues from Defence Research and Development Canada–Valcartier and analyzed in their laboratory.

Water Sample Collection

About 5 m to the right of the rightmost target was a very small intermittent stream that flowed through the edge of the antitank range before disappearing into the soil (Fig. 7). A water sample was collected here by placing a 500-mL amber glass bottle in the stream at a point where the water flowed over a small ledge. The sample was not filtered, and it was maintained at 4°C until extraction.

Soil Sample Analysis

Soil samples were returned to CRREL and air-dried at room temperature. The discrete and composite samples were processed differently because the sample masses were quite different.

Discrete samples were dried in the 4-oz. amber containers, passed through a #10 (2-mm) sieve to remove oversize material, and returned to the 4-oz. containers. Discrete samples were not subsampled; the entire sample was extracted as follows. A volume of acetonitrile in mL, approximately double the mass of the sample in grams, was added to each 4-oz. jar unless the sample was too large. For those cases the sample was transferred to an 8-oz. jar and acetonitrile was added. All jars were capped and placed on a tabletop shaker overnight. The samples were removed from the shaker and allowed to settle for at least an hour. Each sample was filtered through a 0.45- μ m Millex FH filter and placed in a 7-mL amber glass vial. Vials were stored in a refrigerator until analyzed.

Composite soil samples were placed on sheets of aluminum foil to air-dry. Small pieces of propellant were occasionally observed in grid composites and minigrad composites from Grid 10. These pieces were removed from the sample prior to sieving. However, no pieces of propellant were removed from the minigrad samples from Grid 3.

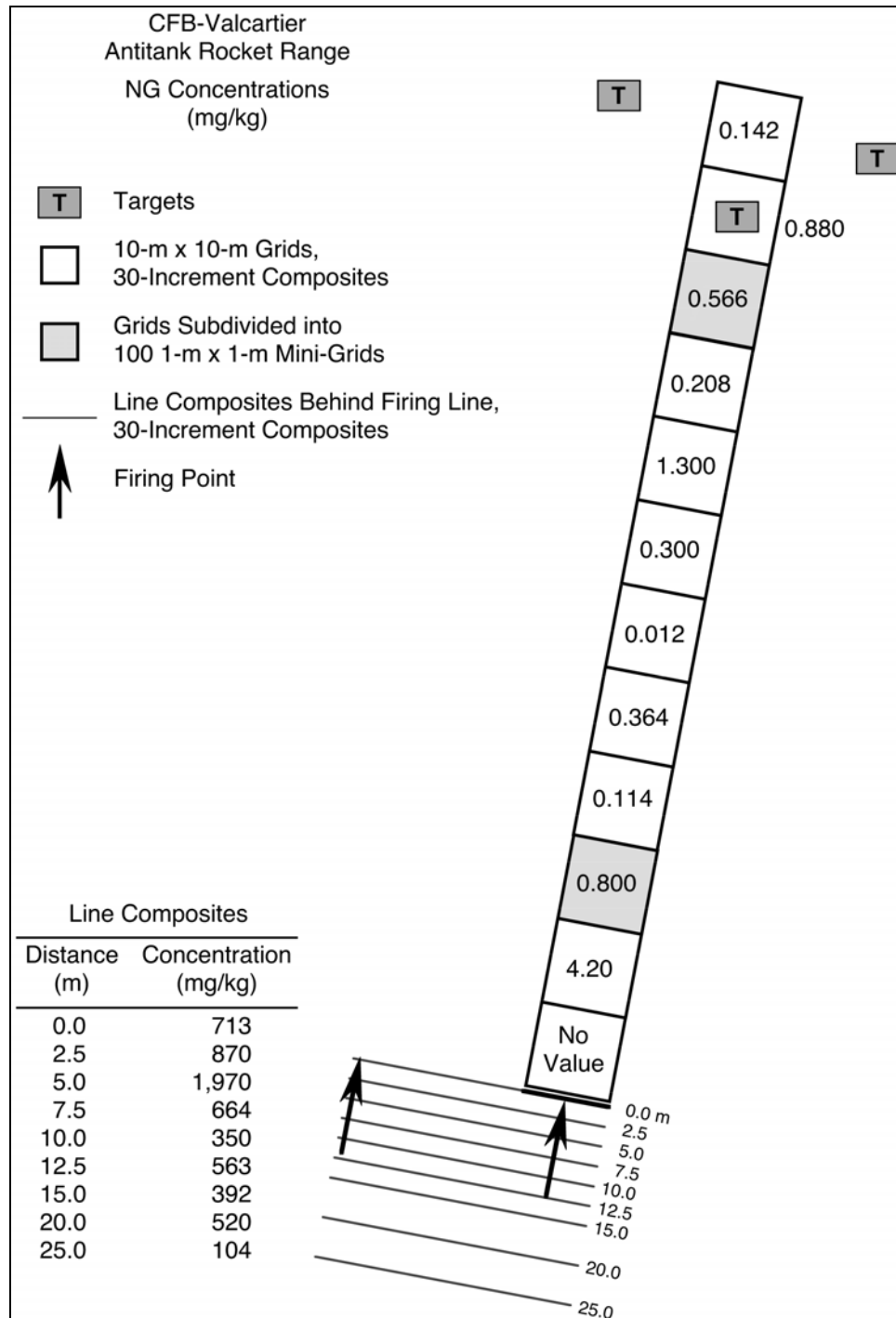


Figure 6. Concentration of NG in composite soil samples collected in front of and behind the rocket firing line.



Figure 7. Intermittent stream at edge of antitank range.

Dried samples were sieved through a #10 sieve (2.00 mm). The material that passed the sieve was ground in a LabTechnics LM2-P (LabTech Essa Pty. Ltd., Bassendean, Western Australia, Australia) puck-mill grinder for 60 seconds. After grinding, composite samples were returned to their original containers and then spread in a thin layer on clean aluminum foil. A subsample was obtained for each composite sample by collecting at least 30 increments randomly from the layer of ground soil for a mass of about 10 g. For every tenth sample, two additional replicate subsamples were collected in an identical manner to enable an assessment of subsampling uncertainty. Each 10-g subsample was extracted with 20 mL of acetonitrile in an ultrasonic bath overnight at room temperature. After sonication, samples were removed from the bath and allowed to settle for at least an hour. An aliquot was then removed, filtered, and placed in a 7-mL amber vial for storage in a refrigerator.

The extracts from both the discrete and composite samples were all analyzed using the general procedures of SW 846 Method 8330 (EPA 1994). For this analysis, an aliquot of each sample was diluted 1 to 4 with reagent-grade water. Analysis was conducted on a modular RP-HPLC system from Thermo Finnigan composed of a SpectraSYSTEM Model P1000 isocratic pump, a SpectraSYSTEM UV2000 dual wavelength UV/VS absorbance detector set at 210 and 254 nm (cell path 1 cm), and a SpectraSYSTEM AS300 autosampler. Samples were introduced by overfilling a 100- μ L sampling loop. Separations were made on a

15-cm \times 3.9-mm (4- μ m) NovaPak C-8 column (Waters Chromatography Division, Milford, Massachusetts) eluted with 15:85 isopropanol/water (v/v) at 1.4 mL/min. Concentrations were estimated against commercial multianalyte standards (Restek) from peak heights. If concentrations exceeded 20 ppm, an aliquot of the original extract was diluted appropriately with additional acetonitrile prior to the 1-to-4 dilution with reagent-grade water. Estimates of detection limits for the target analytes for this method are given in Table 1.

Analyte	Soil, $\mu\text{g kg}^{-1}$		Water, $\mu\text{g L}^{-1}$
	RP-HPLC	GC-ECD	GC-ECD
HMX	26	26	0.047
RDX	34	3	0.035
1,3,5-TNB	16	3	
TNT	16	1	0.017
2,6DNT	19	0.8	
2,4DNT	28	0.8	
2ADNT	38	2.5	
4ADNT	32	1.6	
NG	20	20	0.200
3,5-DNA	Co-elutes with NB	2	
1,3-DNB	100	0.7	
Tetryl	600	20	
PETN	500	16	

For low concentration samples, a second analysis was conducted by GC-ECD following the general procedure outlined in SW846 Method 8095 (EPA 1999). These analyses were conducted on an HP 6890 Gas Chromatograph equipped with a micro ECD detector. Direct injection of 1 μ L of soil extract was made into a purged packed inlet port (250°C) equipped with a deactivated Restek Uniliner. Primary separation was conducted on a 6-m- \times 0.53-mm-ID fused-silica column, with a 1.5- μ m film thickness of 5%-(phenyl)-methylsiloxane (Rtx-5 from Restek, Bellefonte, Pennsylvania). The GC oven was temperature-programmed as follows: 100°C for 2 min, 10°C/min ramp to 280°C. The carrier gas was hydrogen at 10 mL/min (linear velocity approximately 90 cm/sec). The ECD detector temperature was 310°C and the makeup gas was nitrogen flowing

at 45 mL/min. If a peak was observed in the retention window for a specific signature compound, the extract was reanalyzed on a confirmation column, 6-m- × 0.53-mm-ID having a 1.5- μ m film thickness of a proprietary polymer (Rtx-TNT-2 from Restek). The GC oven was temperature-programmed as follows: 130°C for 1 min, 10°C/min ramp to 280°C. The carrier gas was helium at 20 mL/min (linear velocity approximately 180 cm/sec) and the nitrogen makeup gas was flowing at 60 mL/min. Inlet and detector temperature were the same as above. Multianalyte standards were purchased from Restek and the instrument was calibrated over five concentration levels. Estimates of the detection limits for the GC-ECD method are given in Table 1.

Water Sample Analysis

The water sample was analyzed in two ways. First the sample was diluted 3 to 4 with acetonitrile and analyzed using the direct method in SW846 Method 8330 using RP-HPLC. In addition, a 200-mL portion of the water sample was passed through a solid-phase extraction cartridge (Porapak RDX, Waters, Corp.) at 10 mL/min. The cartridge was then eluted with 5 mL of acetonitrile and the extract diluted 1 to 4 with reagent-grade water. The diluted extract was analyzed using RP-HPLC-UV as described above for soil samples. Estimates for the detection limits for HMX, RDX, TNT, and NG are given in Table 1.

4 RESULTS

Grid Samples from the Firing Point Past the Central Target

Results from the analysis of 30-increment composite samples from Grids 2 (G2) through 12 (G12) are presented in Table 2. HMX and NG were detected in all surface samples at concentrations ranging from 0.034 to 888 mg/kg and 0.012 to 4.2 mg/kg, respectively. The source of HMX and NG on this range is the main charge and the double-based propellant, respectively, used for the 66-mm M72 rockets fired here. The highest HMX concentrations were located in the grids next to the target. The highest NG concentrations were found near the firing point of the weapon, and at the target, where residual propellant is dispersed upon impact or detonation (Fig. 7).

Although TNT represents 30% of the main charge for the rocket, it was found in the surface soil at concentrations ranging from <d to 8.46 mg/kg, two to three orders of magnitude less than HMX. The low concentrations of TNT relative to HMX have been observed elsewhere at antitank rocket ranges (Jenkins et al. 1997, 1998; Thiboutot et al. 1998; Pennington et al. 2002), and it appears to be due to either more efficient destruction during detonation, or, more likely, faster environmental dissolution and degradation processes for TNT relative to HMX in the soil (Grant et al. 1993, Price et al. 1997, Lynch et al. 2002).

The only other energetic compounds detected in the grid samples were RDX, 2,4-DNT, and the two environmental transformation products of TNT (2ADNT, and 4ADNT). RDX is present in the booster of the M-72 rockets and was found at concentrations ranging from 0.286 to 1.8 mg/kg in the three grids nearest the target. Likewise, 2ADNT and 4ADNT were present in these three target area grids at concentrations ranging from 0.524 to 2.04 mg/kg. 2,4-DNT was detected in only two grids, with concentrations of 0.008 mg/kg in Grid G4 and 0.728 mg/kg in Grid G12.

NG was the only energetic compound detected in the depth samples collected in Grid G2, near the firing point. The NG concentrations were 2.08 mg/kg in the 0- to 2.5-cm sample, 0.418 mg/kg in the 2.5- to 5-cm sample, and less than a detection limit of 0.020 mg/kg in the 5- to 10-cm sample. We interpret these results to indicate that the NG that was detected was present in small pieces of propellant that were deposited over the surface as the rockets were fired. The acetonitrile extraction solvent will remove the NG from these particles during extraction. Over time the NG present in these particles can slowly dissolve at low concentrations in precipitation, but the stability of NG in pore water within the

soil is thought to be very short as a result of hydrolysis reactions (Jenkins et al. 2003).

Table 2. Analytical results for soil samples collected from Grids G2 through G12 and depth samples from Grids G2 and G10 (analysis by GC-ECD [shaded] and RP-HPLC).							
Sample	Soil concentrations (mg/kg)						
Field #	HMX	RDX	TNT	NG	2,4-DNT	2ADNT	4ADNT
10-m x 10-m grid composites (FP at Grid 0, target in Grid 11)							
G2	0.156	<d	<d	4.20	<d	<d	<d
G3	0.160	<d	<d	0.800	<d	<d	<d
G4	0.034	<d	<d	0.114	0.008	<d	<d
G5	0.072	<d	<d	0.364	<d	0.004	0.002
G6	0.276	<d	<d	0.012	<d	0.002	0.002
G7	2.20	<d	<d	0.300	<d	<d	<d
G8	5.18	<d	0.058	1.30	<d	<d	<d
G9	17.0	<d	0.040	0.208	<d	<d	<d
G10	410	0.690	5.02	0.566	<d	0.984	1.01
G11	888	1.80	8.46	0.880	<d	2.02	2.04
G12	320	0.286	6.10	0.142	0.728	0.578	0.524
Depth samples from Grid 2 in front of firing point							
G2 0–2.5 cm	<d	<d	<d	2.079	<d	<d	<d
G2 2.5–5 cm	<d	<d	<d	0.418	<d	<d	<d
G2 5–10 cm	<d	<d	<d	<d	<d	<d	<d
Depth samples from Grid 10 in front of target							
G10 0–2.5 cm	1030	0.944	0.944	<d	<d	<d	<d
G10 2.5–5 cm	17.2	0.060	0.169	<d	0.043	<d	<d
G10 5–10 cm	1.89	0.119	0.049	<d	<d	<d	<d

In depth samples from Grid 10, HMX was present at the highest concentrations of the energetic compounds. The concentration of HMX in the surface 0 to 2.5 cm was 1030 mg/kg, declining to 17.2 mg/kg in the 2.5- to 5-cm sample, and 1.89 mg/kg in the 5- to 10-cm sample. The rapid decline in concentration with depth was found at the Fort Ord antitank range as well (Jenkins et al. 1998). These results indicated that HMX is leaching downward in this sandy soil, but the major source zone is at the surface in the top 5 cm of soil.

RDX and TNT were also detected in the depth samples from Grid 10. Concentrations of these two compounds declined from 0.944 mg/kg in the sample

from 0 to 2.5 cm for both compounds to 0.060 and 0.169 mg/kg at 2.5 to 5.0 cm and 0.119 and 0.049 mg/kg at 5 to 10 cm, respectively.

NG Concentrations Behind the Firing Line

Analytical results for the two sets of line composite samples that were collected behind the firing line are presented in Table 3 and Figure 7. Only NG was detected in these samples. Concentrations were much greater than those collected in the grids between the firing line and the target with values as high as 2,980 mg/kg for samples collected 5 meters behind the firing line (Fig. 7). Even samples collected 25 meters behind the firing line had NG concentrations as high as 202 mg/kg. Clearly the largest accumulation of NG at this range is in the area behind the firing line where residues from the back blast are deposited.

Distance behind FP (m)	Firing position 1		Firing position 2	
	Rep 1*	Rep 2	Rep 1	Rep 2
0	831	950	668	401
2.5	73.7	43.7	1620	1730
5	2980	2940	890	1670
7.5	201	275	1140	1040
10	61.6	58.2	669	608
12.5	87.4	73.7	933	781
15	274	275	449	567
20	60.4	95.9	1060	860
25	6.00	8.40	198	202

* Laboratory replicate.

Grid 3 Results for Discrete Samples from 100 1-m × 1-m Minigrids

Grid 3 was divided into 100 individual 1-m × 1-m minigrids and discrete samples were collected randomly from the surface (0–2.5 cm) in each (Fig. 8). Upon analysis, only NG was consistently detected in these samples (Table 4). For the discrete samples, the values ranged over two orders of magnitude from 0.023 to 3.37 mg/kg. The median of these samples is 0.403 mg/kg and the calculated mean is 0.645, although the mean is not a good statistic to use for this non-Gaussian distribution. There were 72 individual samples where the concentration was below the calculated mean value, indicating that if a single discrete

sample was used to characterize this grid, almost 75 percent of the time it would be lower than the calculated mean.



Figure 8. Discrete and composite soil sampling in Grid 3.

Figure 9 is a histogram of the 100 discrete samples within Grid 3 using a bin size of 0.1 mg/kg. Clearly this distribution is non-Gaussian. A cumulative frequency plot for these samples is shown in Figure 10. The linearity of this plot is a measure of the normality of the distribution and the plot of the discrete data is clearly nonlinear. Figure 11 is a histogram of the data presented using the log of the concentrations. Clearly the log-transformed data is much more normally distributed than the original data. A cumulative frequency plot of the log-transformed data (Fig. 12) appears quite linear, supporting this conclusion.

In Figure 13 we plotted the NG concentrations found in these discrete samples as a function of position within Grid 3. It doesn't appear that there is a strong concentration gradient within this grid, but to further evaluate this, we plotted the mean concentrations within each row versus distance from the edge of the grid (Fig. 14). From this figure it appears that there is a difference of about a factor of 2 in mean concentration from the edge of Grid 3 closest to the target to the edge closest to the firing point. Compared to the two orders of magnitude difference in individual concentrations, though, this small gradient can be neglected in further analysis of these data.

Table 4. Analytical results from RP-HPLC analysis of discrete soil samples from 1-m x 1-m minigrids within Grid G3 near the firing line of antitank rockets.

Sample	Soil concentrations (mg/kg)						
	Field #	HMX	RDY	TNT	NG	2,4-DNT	2ADNT
G3-D1	<d	<d	<d	0.267	<d	<d	<d
G3-D2	<d	<d	<d	0.079	<d	<d	<d
G3-D3	<d	<d	<d	0.023	<d	<d	<d
G3-D4	<d	<d	<d	0.423	<d	<d	<d
G3-D5	<d	<d	<d	0.173	<d	<d	<d
G3-D6	<d	<d	<d	3.37	<d	<d	<d
G3-D7	<d	<d	<d	0.136	<d	<d	<d
G3-D8	<d	<d	<d	0.153	<d	<d	<d
G3-D9	0.086	<d	<d	0.116	<d	<d	<d
G3-D10	<d	<d	<d	0.120	<d	<d	<d
G3-D11	<d	<d	<d	0.077	<d	<d	<d
G3-D12	<d	<d	<d	0.119	<d	<d	<d
G3-D13	<d	<d	<d	0.248	<d	<d	<d
G3-D14	<d	<d	<d	0.167	<d	<d	<d
G3-D15	0.057	<d	<d	0.441	<d	<d	<d
G3-D16	<d	<d	<d	0.280	<d	<d	<d
G3-D17	<d	<d	<d	0.408	<d	<d	<d
G3-D18	0.158	<d	<d	0.367	<d	<d	<d
G3-D19	<d	<d	<d	0.335	<d	<d	<d
G3-D20	<d	<d	<d	0.397	<d	<d	<d
G3-D21	<d	<d	<d	0.139	<d	<d	<d
G3-D22	<d	<d	<d	0.058	<d	<d	<d
G3-D23	0.046	<d	<d	0.326	<d	<d	<d
G3-D24	<d	<d	<d	0.130	<d	<d	<d
G3-D25	<d	<d	<d	0.227	<d	<d	<d
G3-D26	<d	<d	<d	0.805	<d	<d	<d
G3-D27	0.267	<d	<d	0.351	<d	<d	<d
G3-D28	<d	<d	<d	0.500	<d	<d	<d
G3-D29	0.212	<d	<d	2.28	<d	<d	<d
G3-D30	<d	<d	<d	0.075	<d	<d	<d
G3-D31	<d	<d	<d	0.156	<d	<d	<d

Table 4 (cont'd). Analytical results from RP-HPLC analysis of discrete soil samples from 1-m x 1-m minigrids within Grid G3 near the firing line of antitank rockets.

Sample	Soil concentrations (mg/kg)							
	FIELD #	HMX	RDX	TNT	NG	2,4-DNT	2ADNT	4ADNT
G3-D32		<d	<d	<d	0.223	<d	<d	<d
G3-D33		<d	<d	<d	0.226	<d	<d	<d
G3-D34		<d	<d	<d	0.138	<d	<d	<d
G3-D35		<d	<d	<d	0.103	<d	<d	<d
G3-D36		<d	<d	<d	0.080	<d	<d	<d
G3-D37		<d	<d	<d	2.46	<d	<d	<d
G3-D38		<d	<d	<d	0.230	<d	<d	<d
G3-D39		0.236	<d	<d	0.540	<d	<d	<d
G3-D40		<d	<d	<d	0.215	<d	<d	<d
G3-D41		<d	<d	<d	0.661	<d	<d	<d
G3-D42		<d	<d	<d	0.306	<d	<d	<d
G3-D43		<d	<d	<d	0.140	<d	<d	<d
G3-D44		<d	<d	<d	0.324	<d	<d	<d
G3-D45		<d	<d	<d	0.203	<d	<d	<d
G3-D46		<d	<d	<d	0.217	<d	<d	<d
G3-D47		<d	<d	<d	0.550	<d	<d	<d
G3-D48		<d	<d	<d	0.556	<d	<d	<d
G3-D49		0.085	<d	<d	0.502	<d	<d	<d
G3-D50		<d	<d	<d	1.97	<d	<d	<d
G3-D51		<d	<d	<d	0.398	<d	<d	<d
G3-D52		<d	<d	<d	0.737	<d	<d	<d
G3-D53		0.049	<d	<d	0.561	<d	<d	<d
G3-D54		<d	<d	<d	0.292	<d	<d	<d
G3-D55		0.033	<d	<d	2.12	<d	<d	<d
G3-D56		0.083	<d	<d	1.23	<d	<d	<d
G3-D57		<d	<d	<d	0.483	<d	<d	<d
G3-D58		<d	<d	<d	0.818	<d	<d	<d
G3-D59		<d	<d	<d	1.24	<d	<d	<d
G3-D60		<d	<d	<d	1.77	<d	<d	<d
G3-D61		<d	<d	<d	1.78	<d	<d	<d
G3-D62		<d	<d	<d	0.324	<d	<d	<d
G3-D63		0.089	<d	<d	1.97	<d	<d	<d

Table 4 (cont'd).							
Sample	Soil concentrations (mg/kg)						
Field #	HMX	RDY	TNT	NG	2,4-DNT	2ADNT	4ADNT
G3-D64	0.089	<d	<d	1.20	<d	<d	<d
G3-D65	<d	<d	<d	0.555	<d	<d	<d
G3-D66	<d	<d	<d	0.456	<d	<d	<d
G3-D67	<d	<d	<d	0.454	<d	<d	<d
G3-D68	<d	<d	<d	0.386	<d	<d	<d
G3-D69	<d	<d	<d	0.287	<d	<d	<d
G3-D70	<d	<d	<d	0.395	<d	<d	<d
G3-D71	<d	<d	<d	0.280	<d	<d	<d
G3-D72	<d	<d	<d	1.83	<d	<d	<d
G3-D73	<d	<d	<d	0.201	<d	<d	<d
G3-D74	<d	<d	<d	0.336	<d	<d	<d
G3-D75	<d	<d	0.045	0.208	<d	<d	<d
G3-D76	<d	<d	<d	0.457	<d	<d	<d
G3-D77	0.100	<d	<d	0.430	<d	<d	<d
G3-D78	<d	<d	<d	1.01	<d	<d	<d
G3-D79	<d	<d	<d	0.516	<d	<d	<d
G3-D80	<d	<d	<d	0.397	<d	<d	<d
G3-D81	<d	<d	<d	0.260	<d	<d	<d
G3-D82	<d	<d	<d	0.879	<d	<d	<d
G3-D83	<d	<d	<d	1.15	<d	<d	<d
G3-D84	0.059	<d	<d	2.93	<d	<d	<d
G3-D85	<d	<d	<d	0.965	<d	<d	<d
G3-D86	<d	<d	<d	0.432	<d	<d	<d
G3-D87	0.068	<d	<d	0.604	<d	<d	<d
G3-D88	<d	<d	<d	1.02	<d	<d	<d
G3-D89	<d	<d	<d	0.264	<d	<d	<d
G3-D90	0.107	<d	<d	1.54	<d	<d	<d
G3-D91	<d	<d	<d	0.998	<d	<d	<d
G3-D92	0.040	<d	<d	2.47	<d	<d	<d
G3-D93	<d	<d	<d	0.461	<d	<d	<d
G3-D94	<d	<d	<d	0.559	<d	<d	<d
G3-D95	0.065	<d	<d	1.08	<d	<d	<d
G3-D96	<d	<d	<d	0.956	<d	<d	<d

Table 4 (cont'd). Analytical results from RP-HPLC analysis of discrete soil samples from 1-m x 1-m minigrids within Grid G3 near the firing line of antitank rockets.

Sample	Soil concentrations (mg/kg)							
	Field #	HMX	RDX	TNT	NG	2,4-DNT	2ADNT	4ADNT
G3-D97		<d	<d	<d	0.596	<d	<d	<d
G3-D98		<d	<d	<d	0.542	<d	<d	<d
G3-D99		<d	<d	<d	1.06	<d	<d	<d
G3-D100		0.072	<d	<d	0.226	<d	<d	<d
Min					0.023			
Max					3.370			
Median					0.403			
Mean					0.645			
SD					0.671			

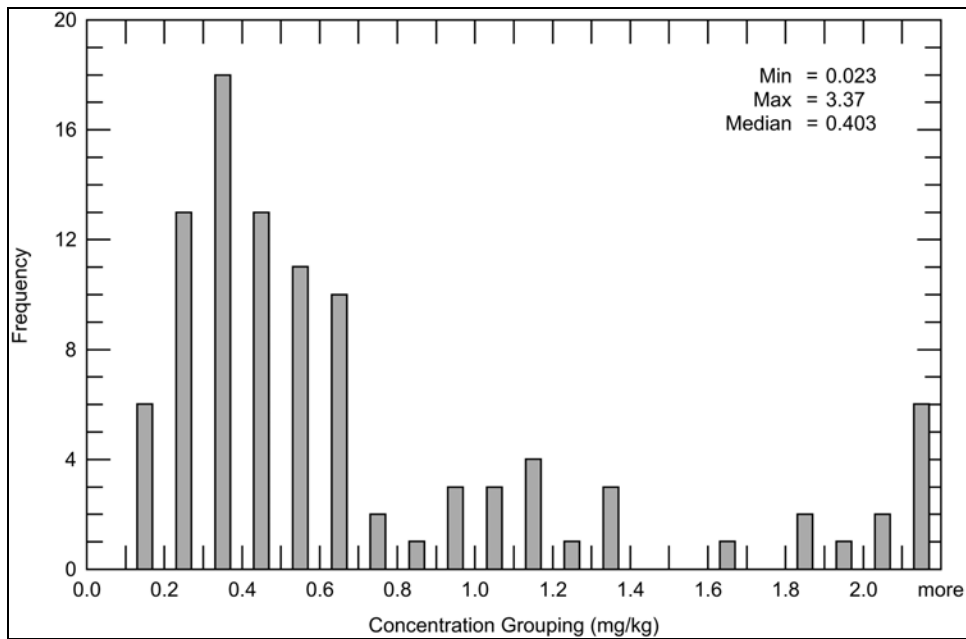


Figure 9. Distribution of NG concentrations for the 100 discrete soil samples collected in Grid 3.

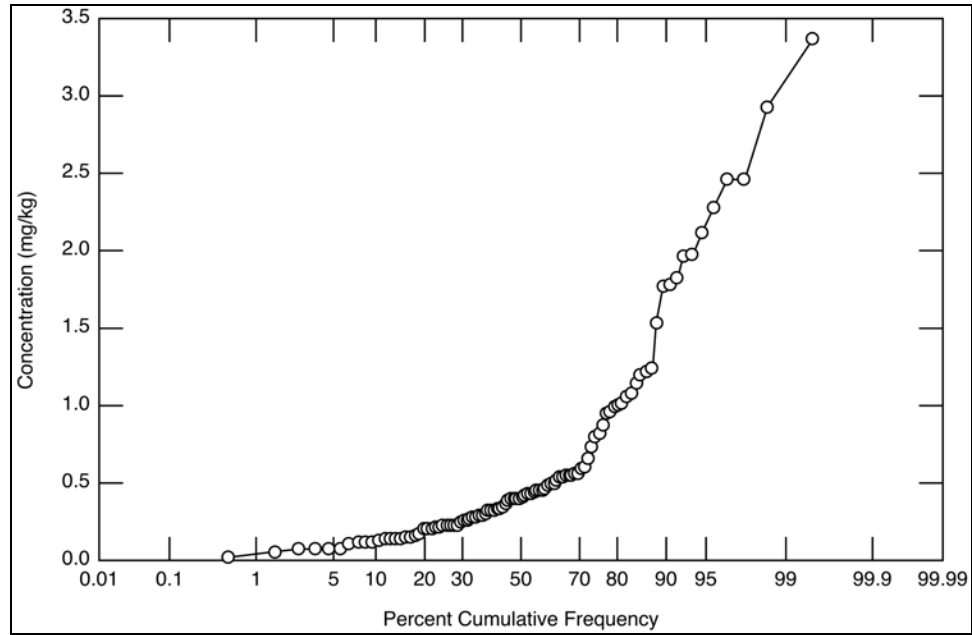


Figure 10. Normal probability plot of NG concentrations in 100 discrete soil samples collected in Grid 3.

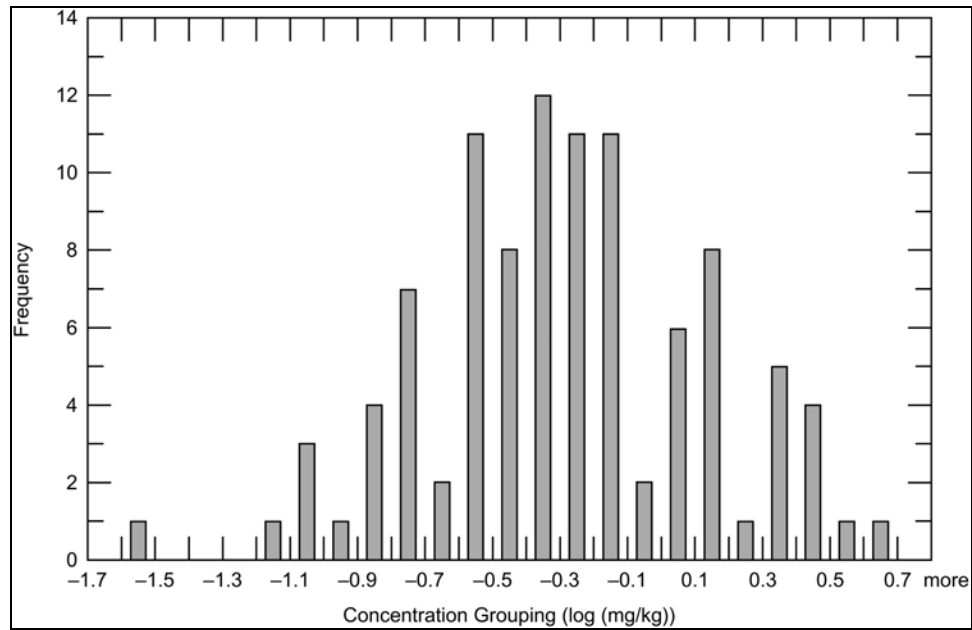


Figure 11. Distribution of the log NG concentrations for 100 discrete soil samples collected in Grid 3.

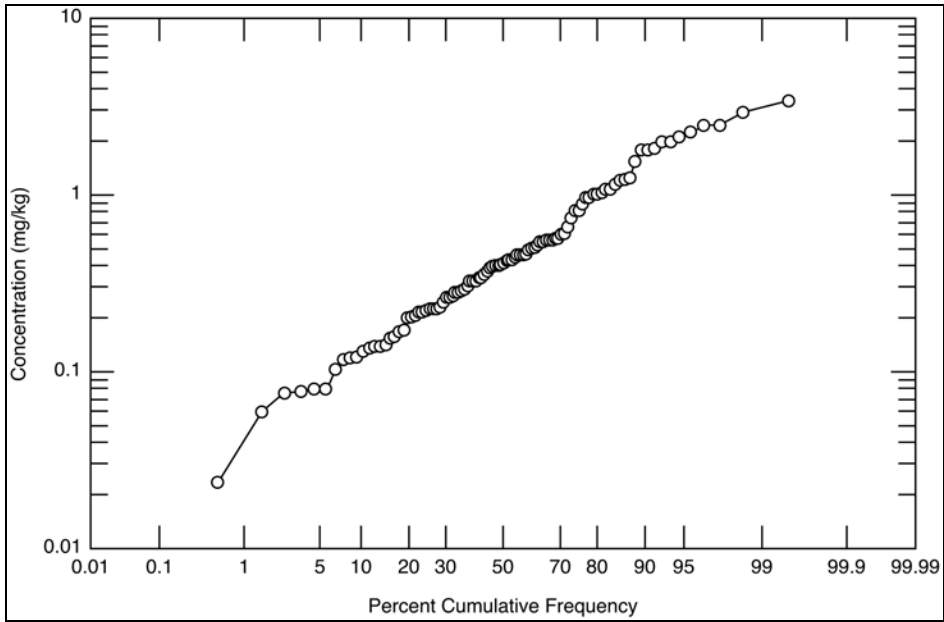


Figure 12. Log normal probability plot of NG concentrations for 100 discrete soil samples from Grid 3.

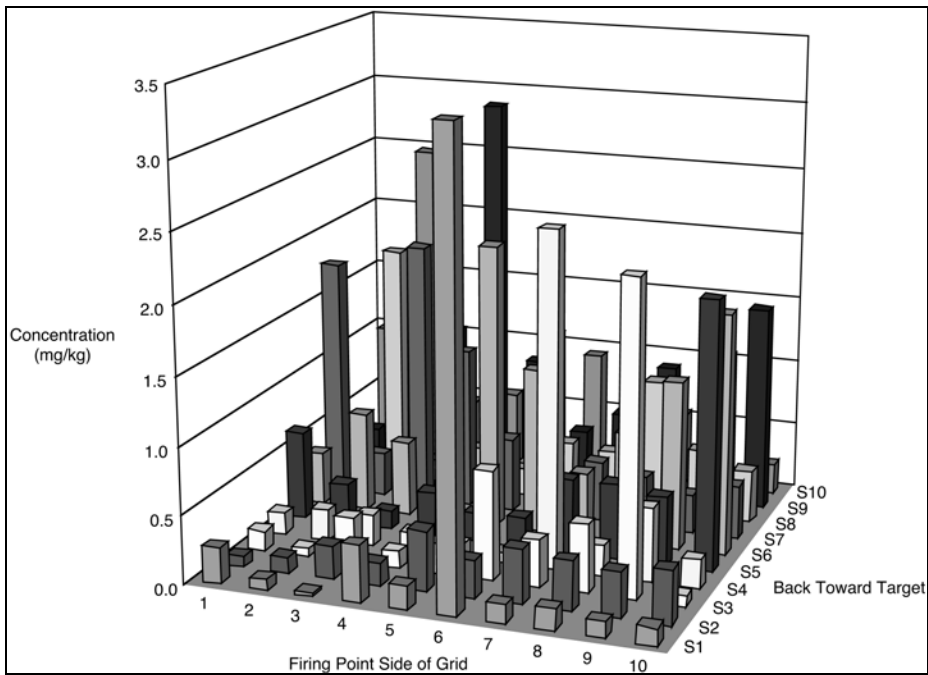


Figure 13. NG concentrations found in discrete samples as a function of position within Grid 3.

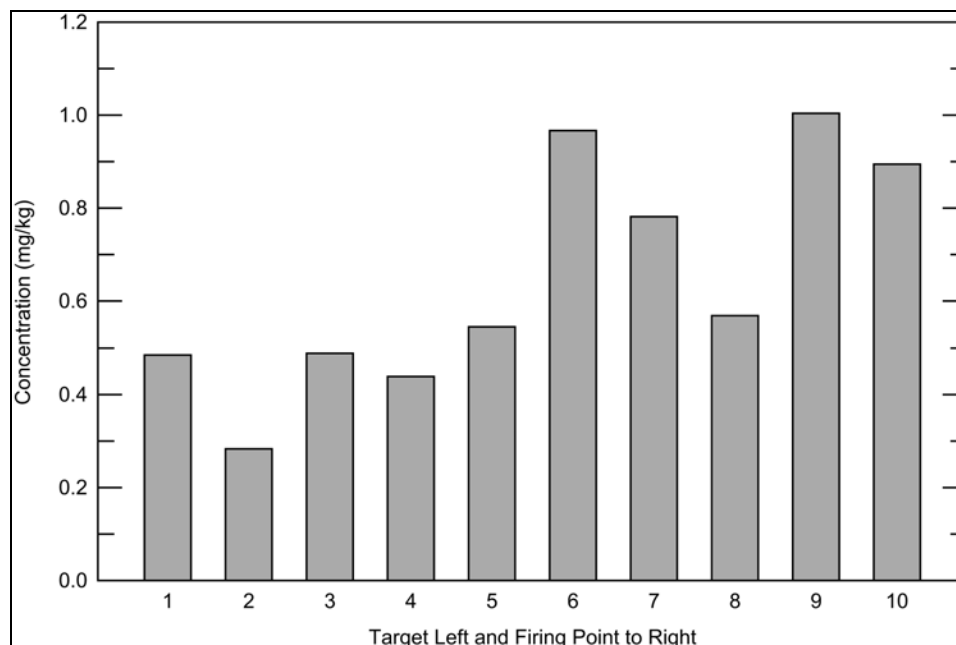


Figure 14. Plot of mean NG concentrations within each row relative to the firing point and target position.

We used this set of 100 discrete samples to evaluate the use of various numbers of individual increments in building multi-increment composite samples. This was done by randomly selecting sets of discrete samples and averaging the results to form mathematical composites. Previous research has demonstrated that whether a set of discrete samples is physically homogenized and a subsample analyzed, or the same discrete samples are individually analyzed and the concentrations averaged, the results are equivalent (Jenkins et al. 1996).

For example, random sets of five discrete concentrations were selected from the fixed set of 100 individual NG concentrations and averaged to simulate 50 multi-increment composite samples with $n = 5$. Removal of individuals from the 100-value data set was done with replacement. The distribution of these data is presented in Figure 15. The range of results is from 0.186 to 1.67 mg/kg or about one order of magnitude, a substantial reduction compared with the range of individual results (Table 5). The mean of this set of 50 five-increment composites is 0.703 mg/kg compared with a mean of 0.645 mg/kg for all 100 individual results.

Similarly, 50 random sets of mathematical composites for values of n of 10, 20, 30, and 50 are presented in Figures 16 to 19; summary statistics from these distributions of composites are presented in Table 5. Clearly, as the number of increments in the composite increases, the range of the distributions narrows and

the distributions appear more and more normal in shape. This is a graphical demonstration of the central limit theorem of statistics, which states that even when a distribution of individual data is non-normal, the distribution of sets of means from this distribution will approximate a normal distribution. Cumulative frequency plots for the $n = 5$ and $n = 30$ distributions are presented in Figure 20. The plot for $n = 30$ is much more linear than that for $n = 5$, confirming that 30 increments provides a more normal distribution than $n = 5$. Another observation from these distributions is that, as the number of increments in the sample increases, the mean and median become closer and closer together (Table 5). This is important because values close to the median value are the most probable values for individual samples.

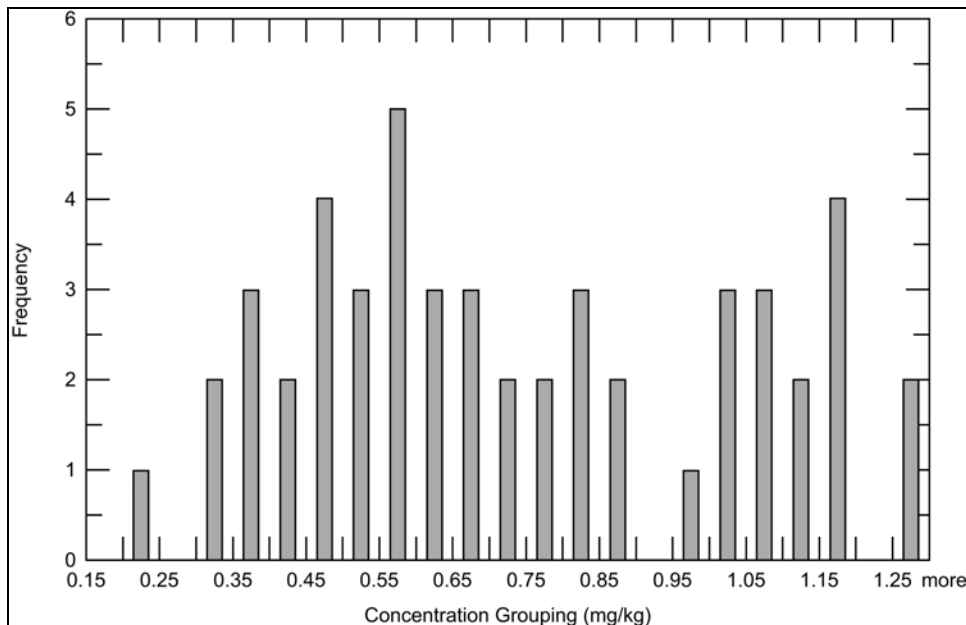


Figure 15. Distribution of NG concentration from mathematically generated (50 times) composites of five increments.

Tolerance intervals (Table 5) were computed for these data sets as $\bar{x} \pm Ks$ where \bar{x} is the mean, s is the standard deviation, and K is the K factor (Natrella 1963). The tolerance ranges were computed by assuming that each computed composite value represented an individual sample. For composite samples of $n = 5$, the minimum and maximum are 0.067 and 1.34 mg/kg, respectively, which still ranges over a factor of 20 from low to high. This indicates that if a 5-increment composite sample was used to estimate the mean for Grid 3, a wide range of values could be obtained. At $n = 30$, though, the tolerance

range is reduced to 0.332 to 0.925 mg/kg, which is less than a factor of 3 from low to high. Certainly the use of a 30-increment composite sample would provide an estimate of the mean concentration in Grid 3 that is much more reliable in terms of representativeness than use of a discrete sample or even a 5-increment composite. The data in Table 5 provide a guide on the uncertainty that is due to the spatial heterogeneity in NG within Grid 3 at the Valcartier antitank range. It also demonstrates the advantage of using a multi-increment composite sample over a discrete sample when the goal is to provide an estimate of the mean concentration for a given area.

Statistics	Number of increments							
		1	5	10	20	30	40	50
Min		0.023	0.19	0.302	0.311	0.344	0.399	0.409
Max		3.37	1.67	1.22	1.04	0.932	0.932	0.828
Median		0.403	0.626	0.630	0.633	0.614	0.675	0.604
Mean		0.645*	0.703	0.628	0.636	0.628	0.674	0.620
SD		*	0.316	0.200	0.182	0.125	0.112	0.105
95% tolerance range [†]	Min	*	-0.050	0.151	0.204	0.332	0.408	0.369
	Max	*	1.46	1.10	1.07	0.925	0.939	0.871

* Inappropriate statistics for a non-Gaussian distribution.
[†] Tolerance range computed as (mean ± K*s) where K is the K factor for 95% confidence that 95% of the individual values will lie within the tolerance range.

Grid 10 Results for Discrete Samples from 100 1-m × 1-m Minigrids

Grid 10 was also subdivided into 100 1-m × 1-m minigrids and sampled in an identical manner as described for Grid 3, except that the depth sampled was 0 to 1.5 cm (Fig. 21). The concentrations obtained for HMX, RDX, TNT, NG, 2ADNT and 4ADNT are presented in Table 6. In general, HMX was present at concentrations two orders of magnitude greater in these samples than for any of the other target analytes with HMX concentrations ranging from 8.33 to 1920 mg/kg. The distribution of these 100 concentrations is again non-Gaussian as shown in Figure 22. The mean concentration for this distribution is 458 mg/kg, the median is 289 mg/kg, and 61 of the 100 individual values are less than the mean. The concentration of the 30-increment composite sample for Grid 10 was 410 mg/kg.

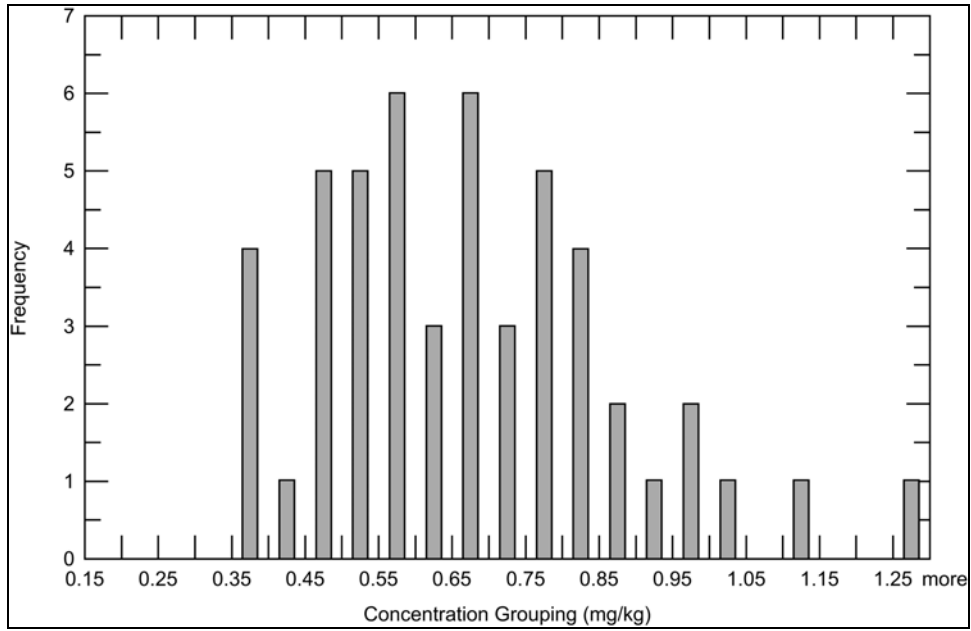


Figure 16. Distribution of NG concentration from mathematically generated (50 times) composites of ten increments.

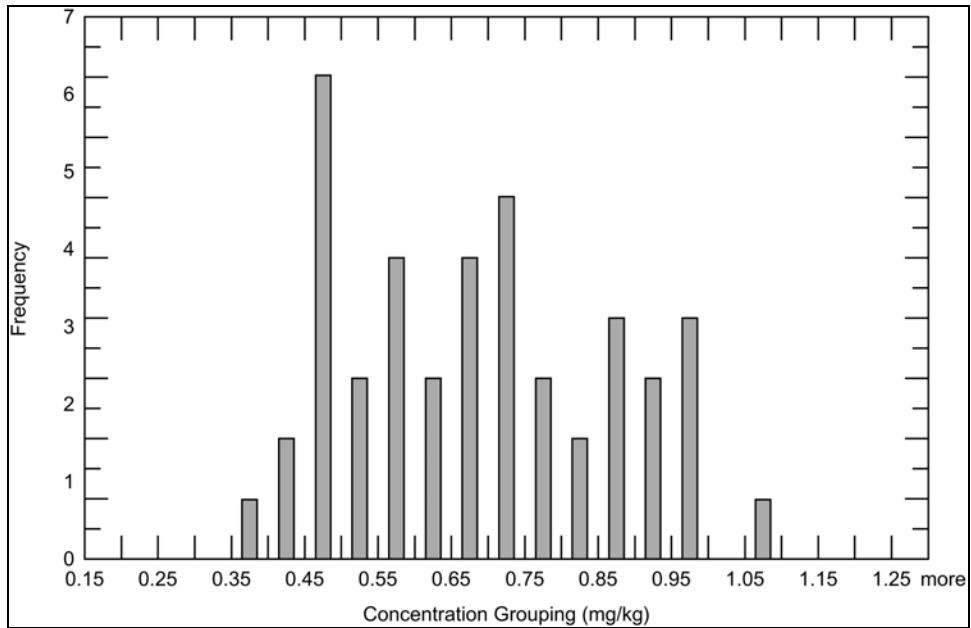


Figure 17. Distribution of NG concentration from mathematically generated (50 times) composites of 20 increments.

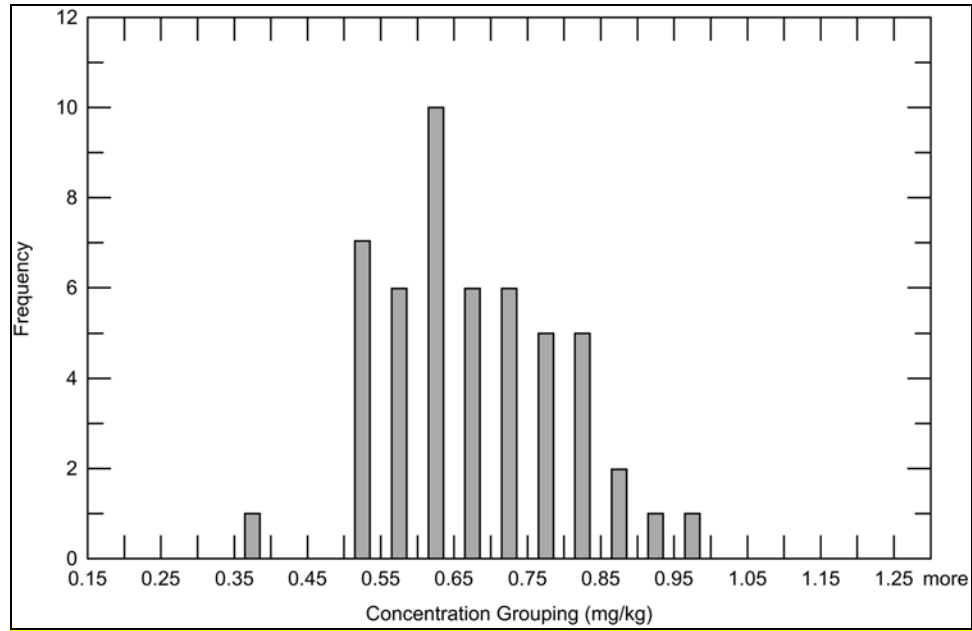


Figure 18. Distribution of NG concentration from mathematically generated (50 times) composites of 30 increments.

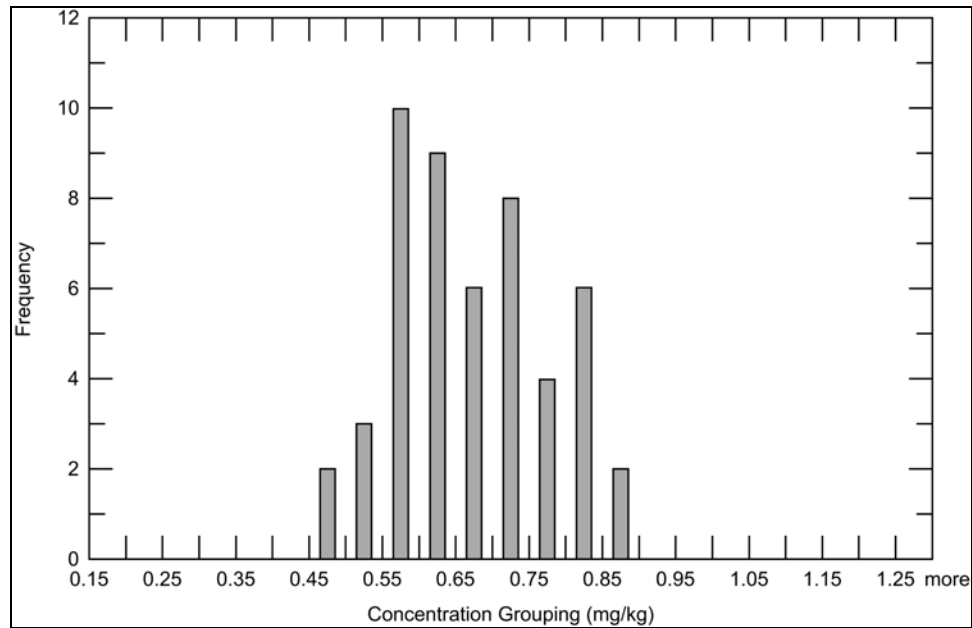


Figure 19. Distribution of NG concentration from mathematically generated (50 times) composites of 50 increments.

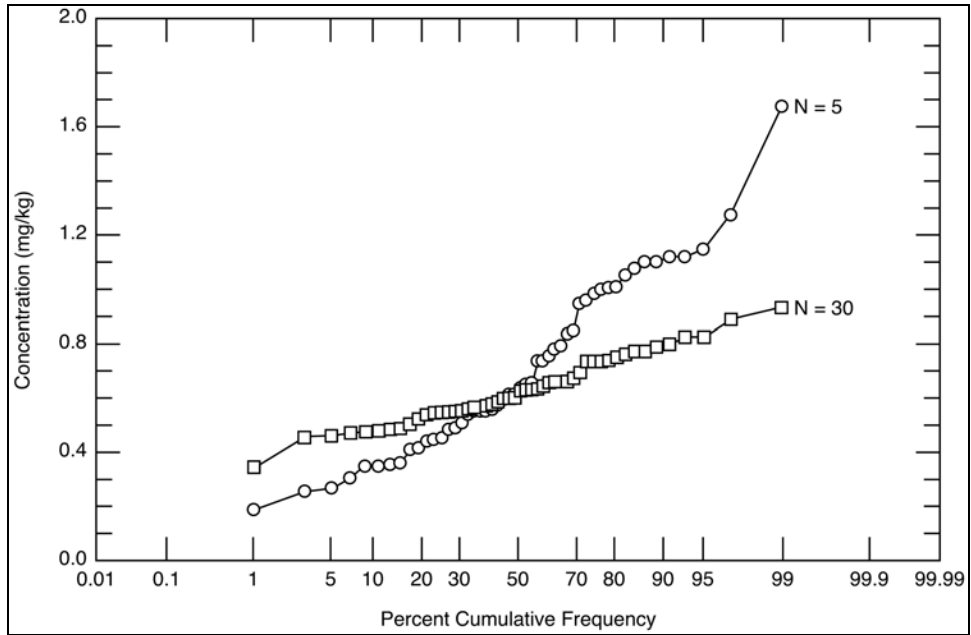


Figure 20. Normal probability plot of NG concentrations from mathematically generated (50 times) composites of 5 and 30 increments.



Figure 21. Collecting discrete and composite soil samples in Grid 10.

Table 6. Analytical results from RP-HPLC analysis of discrete soil samples from 1-m x 1-m minigrids within Grid G10 near a target at the antitank range.

Sample	Soil concentrations, mg/kg					
Field #	HMX	RDX	TNT	NG	2ADNT	4ADNT
G10-D1	936	17.9	52.1	<d	<d	<d
G10-D2	1720	8.72	33.1	<d	<d	<d
G10-D3	1250	<d	23.8	<d	<d	<d
G10-D4	1300	<d	30.9	<d	<d	<d
G10-D5	1050	6.64	18.3	<d	<d	<d
G10-D6	1800	<d	18.8	<d	<d	<d
G10-D7	1920	<d	12.0	<d	<d	<d
G10-D8	1770	4.00	62.0	<d	<d	<d
G10-D9	629	<d	1.53	<d	<d	<d
G10-D10	798	<d	1.19	<d	<d	<d
G10-D11	563	<d	0.796	<d	<d	<d
G10-D12	1620	<d	65.8	<d	<d	<d
G10-D13	987	<d	16.4	<d	<d	<d
G10-D14	46.2	0.192	0.176	<d	<d	<d
G10-D15	645	1.15	0.960	<d	<d	<d
G10-D16	1300	<d	17.4	<d	<d	<d
G10-D17	1100	0.857	2.43	<d	<d	<d
G10-D18	1200	<d	<d	<d	<d	<d
G10-D19	1440	<d	<d	<d	<d	<d
G10-D20	577	3.10	21.7	<d	<d	<d
G10-D21	626	<d	0.587	<d	<d	<d
G10-D22	174	0.138	0.185	<d	<d	<d
G10-D23	638	<d	4.81	<d	<d	<d
G10-D24	994	<d	<d	<d	<d	<d
G10-D25	599	<d	12.5	<d	<d	<d
G10-D26	765	0.643	11.3	<d	<d	<d
G10-D27	868	<d	1.51	<d	<d	<d
G10-D28	419	1.36	1.50	<d	<d	<d
G10-D29	550	<d	1.97	<d	<d	<d
G10-D30	703	<d	0.913	<d	<d	<d
G10-D31	262	<d	<d	<d	<d	<d
G10-D32	295	<d	0.624	<d	<d	<d
G10-D33	231	<d	<d	<d	<d	<d

Table 6 (cont'd). Analytical results from RP-HPLC analysis of discrete soil samples from 1-m x 1-m minigrids within Grid G10 near a target at the antitank range.

Sample	Soil concentrations, mg/kg					
Field #	HMX	RDX	TNT	NG	2ADNT	4ADNT
G10-D34	718	<d	0.872	<d	<d	<d
G10-D35	866	<d	2.79	<d	<d	<d
G10-D36	1110	<d	1.75	<d	<d	<d
G10-D37	842	1.41	2.57	<d	<d	<d
G10-D38	264	<d	0.486	<d	<d	<d
G10-D39	624	<d	0.381	<d	<d	<d
G10-D40	192	<d	0.541	<d	<d	<d
G10-D41	19.9	<d	<d	<d	<d	<d
G10-D42	329	0.688	<d	<d	<d	<d
G10-D43	479	6.33	13.4	<d	<d	<d
G10-D44	674	0.587	1.53	<d	<d	<d
G10-D45	582	<d	2.13	<d	<d	<d
G10-D46	630	<d	21.5	<d	<d	<d
G10-D47	498	0.409	5.18	<d	<d	<d
G10-D48	614	0.453	25.3	<d	<d	<d
G10-D49	156	<d	0.465	<d	<d	<d
G10-D50	34.0	<d	<d	<d	<d	<d
G10-D51	34.3	<d	<d	<d	<d	<d
G10-D52	92.8	<d	<d	<d	<d	<d
G10-D53	159	<d	<d	<d	<d	<d
G10-D54	115	<d	<d	<d	<d	<d
G10-D55	332	0.981	2.94	<d	<d	<d
G10-D56	326	1.29	<d	<d	<d	<d
G10-D57	400	<d	15.0	<d	<d	<d
G10-D58	257	<d	<d	<d	<d	<d
G10-D59	170	0.681	<d	<d	<d	<d
G10-D60	8.33	<d	<d	<d	<d	<d
G10-D61	54.1	<d	<d	<d	<d	<d
G10-D62	26.3	<d	<d	<d	<d	<d
G10-D63	111	<d	<d	<d	<d	<d
G10-D64	381	0.911	<d	<d	<d	<d
G10-D65	60.5	0.735	<d	<d	<d	<d
G10-D66	381	<d	16.8	<d	<d	<d

Table 6 (cont'd).						
Sample	Soil concentrations, mg/kg					
Field #	HMX	RDX	TNT	NG	2ADNT	4ADNT
G10-D67	284	1.88	2.34	<d	<d	<d
G10-D68	283	<d	0.732	<d	<d	<d
G10-D69	177	<d	<d	<d	<d	<d
G10-D70	79.6	<d	6.69	<d	<d	<d
G10-D71	43.3	<d	<d	<d	<d	<d
G10-D72	36.0	<d	0.411	<d	<d	<d
G10-D73	28.1	<d	<d	<d	<d	<d
G10-D74	139	<d	<d	<d	<d	<d
G10-D75	185	<d	<d	<d	<d	<d
G10-D76	27.8	<d	<d	<d	<d	<d
G10-D77	450	0.923	24.7	<d	<d	<d
G10-D78	171	<d	<d	<d	<d	<d
G10-D79	113	<d	<d	<d	<d	<d
G10-D80	53.2	<d	<d	<d	<d	<d
G10-D81	60.8	<d	<d	<d	<d	<d
G10-D82	11.5	<d	<d	<d	<d	<d
G10-D83	83.7	<d	<d	<d	<d	<d
G10-D84	75.5	<d	<d	<d	<d	<d
G10-D85	112	<d	<d	<d	<d	<d
G10-D86	85.9	<d	<d	<d	<d	<d
G10-D87	40.9	<d	<d	<d	<d	<d
G10-D88	28.9	<d	<d	<d	<d	<d
G10-D89	136	<d	1.01	<d	<d	<d
G10-D90	58.3	1.38	<d	<d	<d	<d
G10-D91	93.7	<d	<d	<d	<d	<d
G10-D92	153	<d	<d	<d	<d	<d
G10-D93	75.8	6.64	<d	<d	<d	<d
G10-D94	323	<d	12.4	<d	<d	<d
G10-D95	297	<d	0.533	<d	<d	<d
G10-D96	637	<d	<d	<d	<d	<d
G10-D97	78.0	<d	<d	<d	<d	<d
G10-D98	24.7	<d	<d	<d	<d	<d
G10-D99	73.8	<d	<d	<d	<d	<d

Table 6 (cont'd). Analytical results from RP-HPLC analysis of discrete soil samples from 1-m × 1-m minigrids within Grid G10 near a target at the antitank range.

Sample	Soil concentrations, mg/kg					
Field #	HMX	RDX	TNT	NG	2ADNT	4ADNT
G10-D100	13.8	<d	<d	<d	<d	<d
Min	8					
Max	1920					
Median	289					
Mean	458					
SD	471					

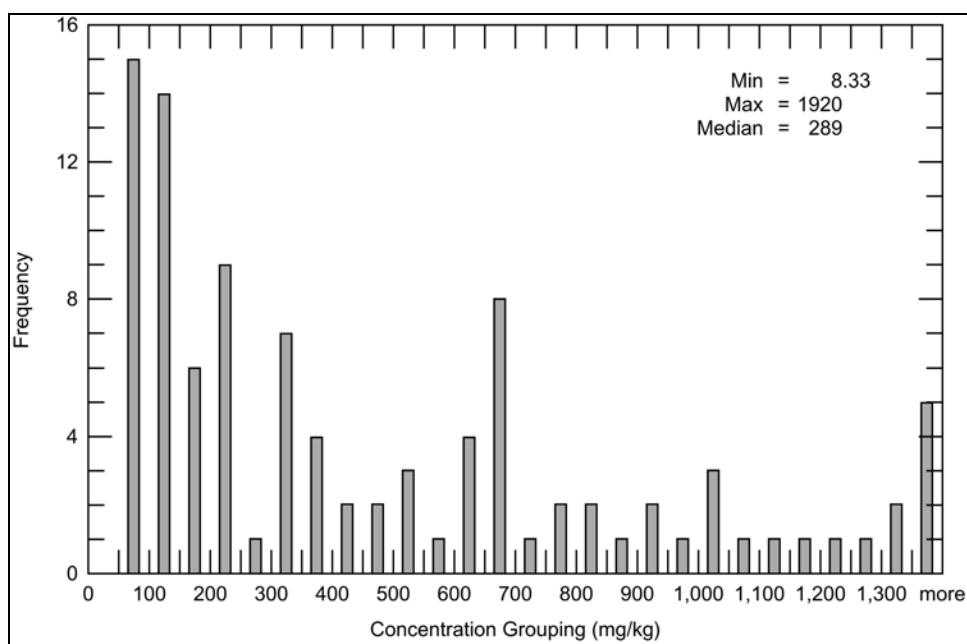


Figure 22. Distribution of HMX concentrations found in 100 discrete soil samples collected in Grid 10.

Figure 23 is a plot of the HMX concentrations as a function of position within the 10-m × 10-m grid. From this plot it appears that there is a strong concentration gradient within the grid, and this was confirmed when we plotted the mean concentrations for each row versus the distance from the edge of the grid (Fig. 24).

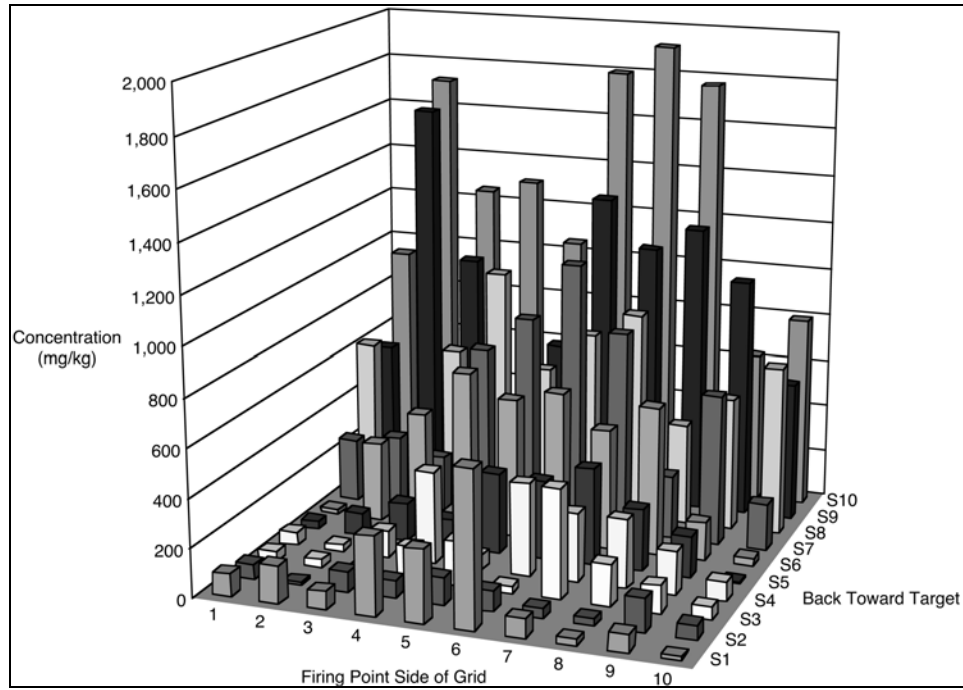


Figure 23. Plot of HMX concentrations as a function of position within Grid 10.

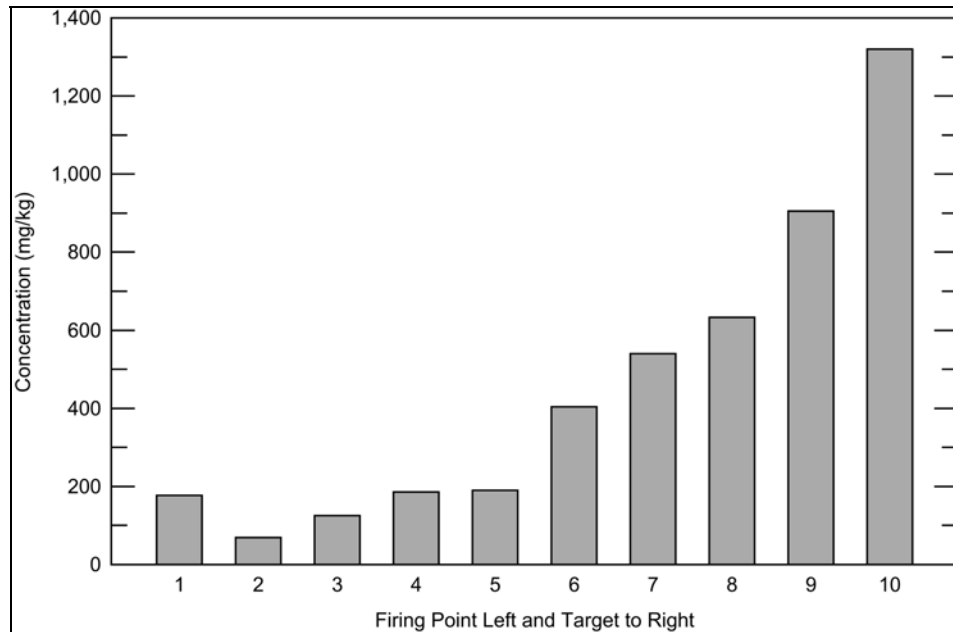


Figure 24. Plot of mean HMX concentrations within each row relative to the firing point and target position.

Clearly dividing up the area near the target in 10-m \times 10-m square grids is not appropriate to characterize an area where a strong gradient is expected. This type of strong concentration gradient for HMX near the target was also found in two other studies of antitank ranges (Jenkins et al. 1997, 1998; Thiboutot et al. 1998) and led to a recommendation of the use of a concentric ring sampling pattern (Fig. 2) for this type of site (Jenkins et al. 1998).

Nevertheless, an area chosen to be characterized may often encompass an area with an unexpected concentration gradient. To demonstrate that even under these circumstances the use of a composite sampling approach can be effective, we used the Grid 10 HMX data to generate computed multi-increment composites as described above for NG in Grid 3. This was done with a goal of evaluating alternatives for obtaining reliable estimates of the average concentration in the 10-m \times 10-m grid. Results for values of n from 5 to 50 are presented in Table 7. The distribution that we obtained for 50 trails with n = 5 and n = 30 are presented in Figures 25 and 26, respectively. For n = 5, the resulting distribution is clearly non-Gaussian with individual composites ranging in concentration from 112 to 876 mg/kg. For n = 30, the distribution appears to be more normal with the range of individual composites ranging from 286 to 644 mg/kg. The 95% tolerance range for n = 5 is -22.1 to 893 mg/kg; the 95% tolerance range for n = 30 is 242 to 655 mg/kg. Thus a much more reliable estimate of the mean concentration for this grid is obtained using a 30-increment composite sample rather than either a single discrete sample or a 5-increment composite.

Table 7. Soil HMX concentrations (mg/kg) from mathematical composites of varying number of increments.

Statistics	Number of increments							
		1	5	10	20	30	40	50
Min		8.33	112	103	220	286	302	287
Max		1,920	876	741	661	644	580	600
Median		289	402	389	409	440	468	415
Mean		*	435	402	424	449	451	432
SD		*	192	140	105	87	74	76
95% tolerance range [†]	Min	*	-22.1	69.9	173	242	276	251
	Max	*	893	735	674	655	626	613

* Inappropriate statistics for a non-Gaussian distribution.
[†] Tolerance range computed as (mean \pm K*s) where K is the K factor for 95% confidence that 95% of the individual values will lie within the tolerance range.

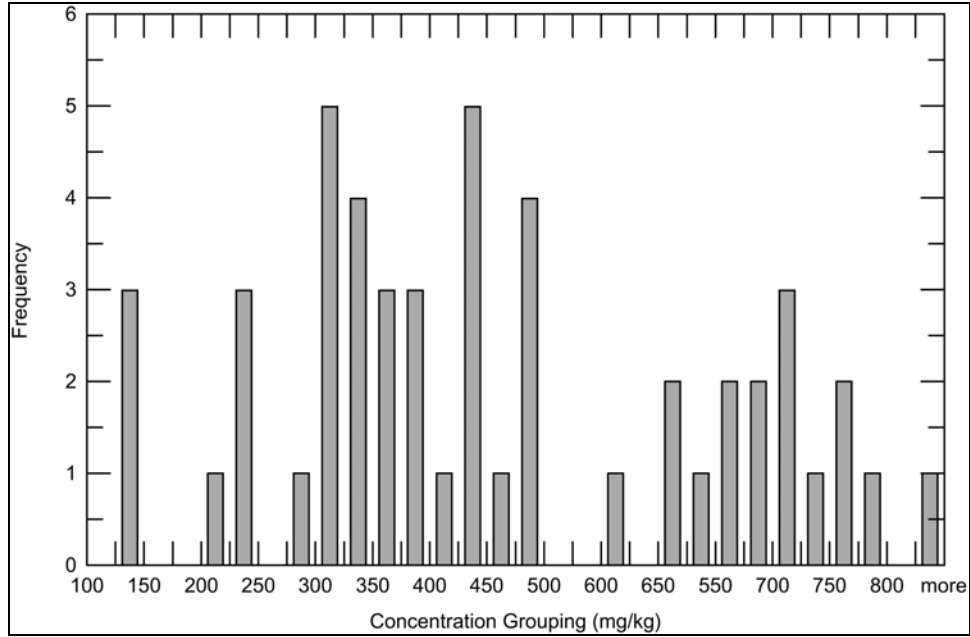


Figure 25. Distribution of HMX concentrations from mathematically generated (50 times) composites of five increments.

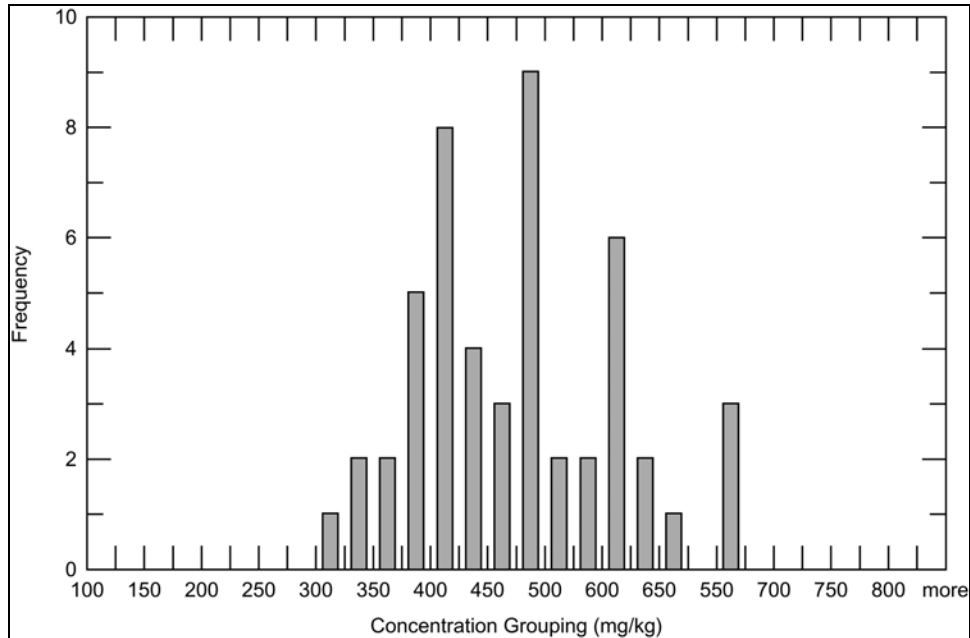


Figure 26. Distribution of HMX concentrations from mathematically generated (50 times) composites of 30 increments.

Comparison of Discrete and 10-Increment Composite Samples for Grids 3 and 10

In addition to the discrete samples collected in each of the 100 minigrids within Grid 3 and 10, 10-increment composite samples were also collected from each of these minigrids (Tables 8 and 9). We estimate the surface area sampled using the 10-increment composites was about 5% of the total surface area of each minigrid whereas the discrete samples sampled about 0.5% of the surface. Thus the composite samples should be a better estimate of the mean concentration for each minigrid based on sampling considerations alone.

The pairs of concentrations obtained for the discrete and composite samples for each of the 100 minigrids are plotted for NG in Grid 3 in Figure 27. The correlation for these pairs of NG data in Grid 3 is very poor ($R^2=0.013$). We eliminated the five pairs of data that had the greatest differences, assuming that these discrepancies may have been due to the presence of a small particle of propellant in the portion of the sample that was extracted, and correlated the data again in Figure 28. The correlation coefficient improved slightly ($R^2 = 0.036$), but the correlation was still very poor. This result is consistent with the very large short-range heterogeneity demonstrated in earlier work for HMX at antitank ranges (Jenkins et al. 1997). Thus, a single discrete sample is not a good representative sample even for a surface area as small as 1 m².

The pairs of concentrations for HMX in the set of 100 minigrids for Grid 10 were treated in a similar manner. A correlation of the 100 pairs of data is presented in Figure 29. The correlation coefficient for this data ($R^2 = 0.781$) is much greater than found for NG in Grid 3, and the low random error variance resulted in the detection of a significant difference between the two populations using a paired t-test at the 95% confidence level. The slope of the correlation was 0.755 (Fig. 29), indicating that the concentrations obtained for the composite samples were biased low compared with the discrete samples. This bias, however, is quite small compared with other contributions to other sources of uncertainty, but additional research will be conducted to try to understand the cause.

Results from Halo Sampling Pattern Around Central Target

The analytical results for the surface soil samples collected using the sampling strategy developed by Ampleman et al. (2003a, b) around the central target are presented in Table 10. The following seven target analytes were detected in these samples in order of decreasing concentrations: HMX, NG, TNT, RDX, 4ADNT, 2ADNT, and 2,4-DNT.

Sample	Soil concentrations, mg/kg						
Field #	HMX	RDY	TNT	NG	2,4-DNT	2ADNT	4ADNT
G3-C1	0.026	<d	0.004	0.134	<d	<d	<d
G3-C2	0.030	<d	<d	0.152	<d	<d	<d
G3-C3	0.030	<d	<d	0.124	<d	<d	<d
G3-C4	<d	<d	<d	0.232	<d	<d	<d
G3-C5	<d	<d	0.002	0.148	<d	<d	<d
G3-C6	0.05	<d	<d	0.122	<d	<d	<d
G3-C7	<d	<d	<d	0.246	<d	<d	<d
G3-C8	0.046	<d	<d	0.296	<d	<d	<d
G3-C9	<d	<d	0.004	0.090	<d	0.002	0.002
G3-C10	0.116	<d	<d	13.1	<d	<d	<d
G3-C11	<d	<d	<d	0.298	<d	<d	<d
G3-C12	<d	<d	<d	0.210	<d	<d	<d
G3-C13	<d	<d	0.004	0.174	<d	<d	<d
G3-C14	0.028	0.004	0.01	0.138	<d	0.002	0.002
G3-C15	<d	<d	<d	0.246	<d	<d	<d
G3-C16	<d	0.004	0.012	0.150	<d	<d	<d
G3-C17	<d	<d	0.004	0.156	<d	<d	<d
G3-C18	<d	<d	0.002	0.172	<d	<d	<d
G3-C19	0.036	<d	<d	0.138	<d	<d	<d
G3-C20	0.052	<d	<d	0.610	<d	<d	<d
G3-C21	<d	<d	<d	0.626	<d	<d	<d
G3-C22	0.008	<d	<d	0.198	<d	<d	<d
G3-C23	<d	<d	<d	0.300	<d	0.004	0.002
G3-C24	<d	<d	<d	0.106	<d	<d	<d
G3-C25	<d	<d	0.002	0.160	<d	<d	<d
G3-C26	<d	<d	0.002	0.282	<d	<d	<d
G3-C27	<d	<d	0.002	0.316	<d	<d	<d
G3-C28	<d	<d	0.004	0.242	<d	<d	<d
G3-C29	0.060	<d	<d	0.526	<d	<d	<d
G3-C30	0.050	<d	<d	0.474	<d	<d	<d
G3-C31	<d	<d	<d	0.280	<d	<d	<d
G3-C32	<d	<d	<d	0.160	<d	<d	<d
G3-C33	<d	<d	<d	0.632	<d	<d	<d
G3-C34	<d	<d	<d	0.426	<d	0.004	0.002
G3-C35	<d	<d	<d	0.104	<d	<d	<d

Table 8 (cont'd). Soil concentrations, Grid 3 (100 10-increment composite samples from 1-m × 1-m minigrids) (analysis by GC-ECD [shaded] and RP-HPLC).

Sample	Soil concentrations, mg/kg						
Field #	HMX	RDX	TNT	NG	2,4-DNT	2ADNT	4ADNT
G3-C36	<d	<d	<d	0.266	<d	<d	<d
G3-C37	<d	<d	<d	0.478	<d	<d	<d
G3-C38	<d	<d	<d	0.776	<d	<d	<d
G3-C39	<d	<d	<d	0.83	<d	<d	<d
G3-C40	0.038	<d	<d	0.378	<d	<d	<d
G3-C41	0.024	0.004	<d	0.260	<d	<d	<d
G3-C42	<d	<d	0.006	0.130	<d	<d	<d
G3-C43	<d	<d	<d	0.726	<d	<d	<d
G3-C44	<d	<d	0.004	0.284	<d	0.004	0.002
G3-C45	0.048	<d	<d	0.428	<d	<d	<d
G3-C46	<d	<d	0.006	0.188	<d	<d	<d
G3-C47	<d	<d	0.004	0.254	<d	0.002	0.002
G3-C48	0.106	<d	0.004	0.286	<d	<d	<d
G3-C49	0.182	<d	<d	0.506	<d	<d	<d
G3-C50	0.118	<d	0.008	0.394	<d	0.002	0.002
G3-C51	0.042	<d	<d	1.63	<d	<d	<d
G3-C52	<d	<d	0.002	0.408	<d	<d	<d
G3-C53	<d	<d	<d	0.824	<d	<d	<d
G3-C54	0.038	<d	0.004	0.182	<d	<d	<d
G3-C55	<d	<d	<d	0.960	<d	<d	<d
G3-C56	<d	<d	<d	0.404	0.010	<d	<d
G3-C57	<d	<d	<d	0.626	<d	<d	<d
G3-C58	0.040	<d	<d	0.458	<d	<d	<d
G3-C59	0.046	<d	<d	0.748	<d	<d	<d
G3-C60	0.262	<d	0.01	0.478	<d	<d	<d
G3-C61	<d	<d	<d	0.980	<d	<d	<d
G3-C62	<d	<d	<d	1.96	<d	<d	<d
G3-C63	<d	<d	<d	0.252	<d	0.004	0.004
G3-C64	<d	<d	<d	0.500	<d	<d	<d
G3-C65	<d	<d	<d	1.35	<d	<d	<d
G3-C66	0.056	<d	<d	0.464	<d	<d	<d
G3-C67	<d	<d	<d	0.358	<d	0.004	0.004
G3-C68	<d	<d	<d	0.984	<d	<d	<d
G3-C69	0.080	<d	<d	0.454	<d	<d	<d
G3-C70	0.042	<d	<d	0.582	<d	<d	<d

Sample	Soil concentrations, mg/kg						
Field #	HMX	RDx	TNT	NG	2,4-DNT	2ADNT	4ADNT
G3-C71	<d	<d	<d	0.442	<d	<d	<d
G3-C72	<d	<d	<d	4.86	<d	<d	<d
G3-C73	<d	<d	<d	0.63	<d	<d	<d
G3-C74	<d	<d	<d	0.352	<d	<d	<d
G3-C75	<d	<d	<d	0.292	<d	<d	<d
G3-C76	<d	<d	<d	0.520	<d	<d	<d
G3-C77	<d	<d	<d	0.202	<d	<d	<d
G3-C78	<d	<d	<d	0.556	<d	<d	<d
G3-C79	<d	<d	<d	0.530	<d	<d	<d
G3-C80	0.150	<d	<d	0.608	<d	<d	<d
G3-C81	<d	<d	<d	1.67	<d	<d	<d
G3-C82	<d	<d	<d	1.43	<d	<d	<d
G3-C83	<d	<d	<d	1.61	<d	<d	<d
G3-C84	<d	<d	<d	3.86	<d	<d	<d
G3-C85	0.028	<d	<d	0.244	<d	0.002	0.002
G3-C86	<d	<d	<d	1.62	<d	<d	<d
G3-C87	<d	<d	<d	0.346	<d	<d	<d
G3-C88	<d	<d	<d	0.464	<d	<d	<d
G3-C89	0.206	<d	<d	0.358	<d	<d	<d
G3-C90	<d	<d	<d	0.532	<d	<d	<d
G3-C91	0.026	<d	<d	0.978	<d	<d	<d
G3-C92	<d	<d	<d	0.414	<d	<d	<d
G3-C93	0.088	<d	<d	0.522	<d	<d	<d
G3-C94	<d	<d	<d	0.950	<d	<d	<d
G3-C95	<d	<d	<d	6.72	<d	<d	<d
G3-C96	<d	<d	<d	0.900	<d	<d	<d
G3-C97	<d	<d	<d	0.610	<d	<d	<d
G3-C98	<d	<d	<d	0.534	<d	<d	<d
G3-C99	<d	<d	<d	0.508	<d	<d	<d
G3-C100	0.090	<d	<d	0.378	<d	<d	<d
			Min	0.09			
			Max	13.12			
			Mean	0.76216			
			Median	0.42			
			SD	1.543			

Table 9. Soil concentrations, Grid 10 (100 10-increment composite samples from 1-m x 1-m minigrids) (analysis by RP-HPLC).

Sample	Soil concentrations, (mg/kg)						
	Field #	HMX	RDX	TNT	NG	2,4-DNT	2ADNT
G10-C1	776	<d	6.40	<d	<d	<d	<d
G10-C2	1120	<d	16.2	11.8	<d	<d	<d
G10-C3	1080	<d	10.0	<d	<d	<d	<d
G10-C4	1210	4.40	11.0	4.80	<d	<d	<d
G10-C5	868	<d	<d	10.6	<d	<d	<d
G10-C6	1400	<d	8.60	6.60	<d	<d	<d
G10-C7	1520	<d	11.4	3.40	<d	<d	<d
G10-C8	1500	24.8	13.8	<d	<d	<d	<d
G10-C9	1060	<d	5.60	<d	<d	<d	<d
G10-C10	478	<d	<d	<d	<d	<d	<d
G10-C11	386	<d	<d	<d	<d	<d	<d
G10-C12	680	<d	4.60	<d	<d	<d	<d
G10-C13	750	<d	5.40	<d	<d	<d	<d
G10-C14	614	<d	11.8	4.40	<d	<d	<d
G10-C15	752	<d	<d	<d	<d	<d	<d
G10-C16	1080	<d	11.0	<d	<d	<d	<d
G10-C17	1120	<d	10.4	<d	<d	<d	<d
G10-C18	966	<d	4.0	8.00	<d	<d	<d
G10-C19	518	<d	7.20	<d	<d	<d	<d
G10-C20	438	<d	5.00	4.00	<d	<d	<d
G10-C21	226	<d	<d	<d	<d	<d	<d
G10-C22	258	<d	<d	<d	<d	<d	<d
G10-C23	682	<d	4.40	<d	<d	<d	<d
G10-C24	698	<d	6.00	7.80	<d	<d	<d
G10-C25	772	<d	8.00	<d	<d	<d	<d
G10-C26	680	<d	<d	17.4	<d	<d	<d
G10-C27	478	<d	<d	<d	<d	<d	<d
G10-C28	576	<d	<d	<d	<d	<d	<d
G10-C29	374	0.5	1.42	<d	<d	<d	<d
G10-C30	298	<d	8.02	<d	<d	<d	<d
G10-C31	254	<d	1.30	<d	<d	<d	<d
G10-C32	270	<d	1.04	<d	<d	<d	<d
G10-C33	422	2.80	3.78	3.08	<d	<d	<d
G10-C34	778	<d	3.60	7	<d	<d	<d
G10-C35	856	<d	9.40	<d	<d	<d	<d

Sample	Soil concentrations, (mg/kg)						
Field #	HMX	RDX	TNT	NG	2,4-DNT	2ADNT	4ADNT
G10-C36	774	<d	4.60	9	<d	<d	<d
G10-C37	44.4	0.36	0.54	<d	<d	<d	<d
G10-C38	444	0.520	2.10	<d	<d	0.580	0.580
G10-C39	286	0.280	5.36	6.08	<d	0.260	0.380
G10-C40	226	0.060	0.212	0.788	<d	0.214	0.234
G10-C41	83.0	<d	2.52	<d	<d	<d	<d
G10-C42	185	1.32	2.10	<d	<d	<d	<d
G10-C43	236	2.56	3.92	16.8	<d	<d	<d
G10-C44	426	0.820	1.34	3.56	<d	<d	<d
G10-C45	440	0.580	0.880	0.640	<d	0.740	0.600
G10-C46	460	0.400	0.44	8.44	<d	0.620	0.660
G10-C47	402	0.260	2.66	3.32	<d	0.500	0.360
G10-C48	534	<d	0.820	5.24	<d	<d	<d
G10-C49	352	2.34	4.92	10.7	<d	<d	<d
G10-C50	181	<d	<d	<d	<d	<d	<d
G10-C51	32.2	<d	0.312	<d	<d	0.094	<d
G10-C52	99.6	0.078	1.65	7.60	<d	0.154	0.148
G10-C53	148	<d	<d	<d	<d	<d	<d
G10-C54	214	<d	0.100	<d	<d	<d	<d
G10-C55	164	<d	<d	<d	<d	<d	<d
G10-C56	302	<d	5.98	0.660	<d	<d	<d
G10-C57	322	<d	0.940	5.02	<d	<d	<d
G10-C58	314	<d	1.34	1.20	<d	<d	<d
G10-C59	142	<d	1.68	<d	<d	<d	<d
G10-C60	44.8	0.052	0.642	0.290	<d	<d	<d
G10-C61	39.4	<d	1.22	0.056	<d	<d	<d
G10-C62	47.0	<d	0.102	0.194	<d	<d	<d
G10-C63	8.02	<d	<d	<d	<d	<d	<d
G10-C64	218	<d	0.042	<d	<d	<d	<d
G10-C65	191	<d	0.220	<d	<d	<d	<d
G10-C66	127	<d	1.98	<d	<d	<d	<d
G10-C67	234	<d	<d	6.28	<d	<d	<d
G10-C68	182	<d	<d	<d	<d	<d	<d
G10-C69	123	<d	<d	<d	<d	<d	<d
G10-C70	126	0.700	9.42	2.52	<d	<d	<d
G10-C71	39.0	<d	0.554	<d	<d	<d	<d

Table 9 (cont'd). Soil concentrations Grid 10 (100 10-increment composite samples from 1-m x 1-m minigrids) (analysis by RP-HPLC).

Sample	Soil concentrations, (mg/kg)						
Field #	HMX	RDX	TNT	NG	2,4-DNT	2ADNT	4ADNT
G10-C72	56.2	<d	1.34	0.416	<d	<d	<d
G10-C73	77.2	<d	0.5	<d	<d	<d	<d
G10-C74	83.8	<d	<d	0.040	<d	<d	<d
G10-C75	177	<d	<d	<d	<d	<d	<d
G10-C76	177	<d	<d	3.16	<d	<d	<d
G10-C77	150	<d	0.420	3.24	<d	<d	<d
G10-C78	123	<d	<d	0.920	<d	<d	<d
G10-C79	183	<d	1.96	1.06	<d	<d	<d
G10-C80	78.4	<d	0.678	0.324	<d	<d	<d
G10-C81	62.0	0.122	<d	<d	<d	<d	<d
G10-C82	21.0	<d	<d	0.720	<d	<d	<d
G10-C83	63.8	0.046	0.080	0.042	<d	<d	<d
G10-C84	79.0	<d	0.324	<d	<d	<d	<d
G10-C85	112	<d	1.07	1.24	<d	<d	<d
G10-C86	69.4	<d	0.058	<d	<d	<d	<d
G10-C87	40.2	<d	<d	0.092	<d	<d	<d
G10-C88	77.4	<d	1.53	1.30	0.162	0.120	0.124
G10-C89	112	<d	1.50	0.540	<d	<d	<d
G10-C90	23.2	<d	0.054	0.132	<d	<d	<d
G10-C91	127	<d	<d	<d	<d	<d	<d
G10-C92	96.6	<d	1.70	2.28	<d	<d	<d
G10-C93	70.2	<d	1.05	0.874	<d	<d	<d
G10-C94	171	<d	0.420	<d	<d	<d	<d
G10-C95	50.2	<d	1.13	2.48	<d	<d	<d
G10-C96	39.2	<d	0.722	<d	<d	<d	<d
G10-C97	60.4	<d	1.29	0.086	<d	0.112	0.106
G10-C98	67.4	<d	<d	0.326	<d	<d	<d
G10-C99	81.6	<d	0.584	0.160	<d	<d	<d
G10-C100	12.6	<d	<d	0.102	<d	<d	<d
Min	8.02						
Max	1520						
Mean	367						
Median	222						
SD	367						

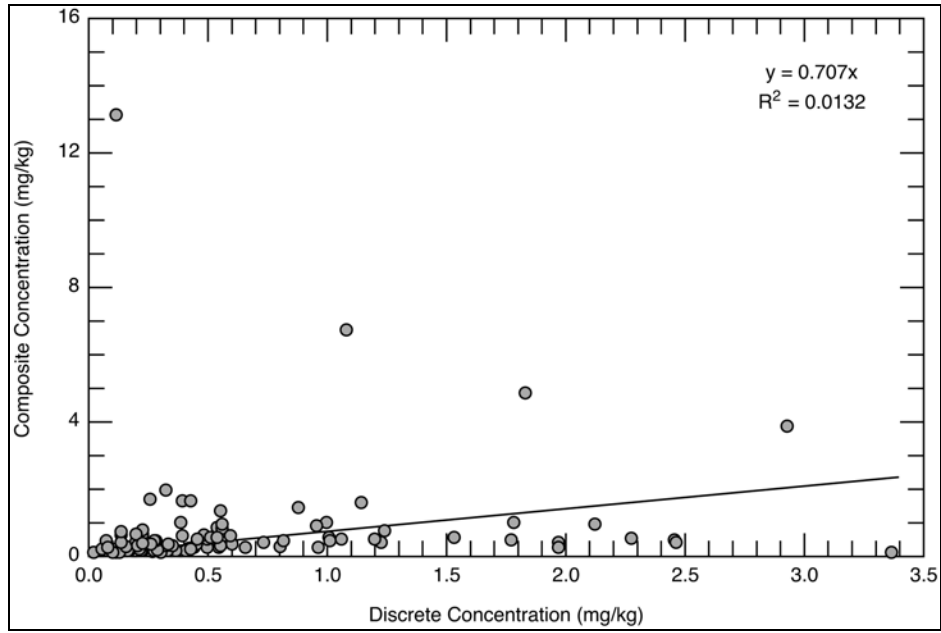


Figure 27. Comparison of NG concentration in discrete and composite soil samples collected in Grid 3.

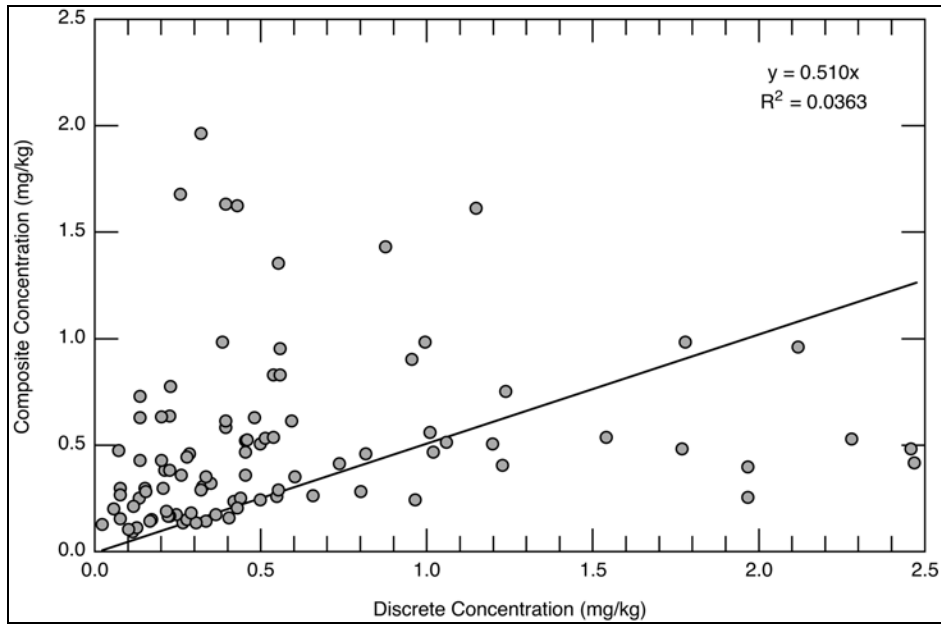


Figure 28. Comparison of NG concentration in discrete and composite soil samples collected in Grid 3, minus the five pairs of data with the greatest differences.

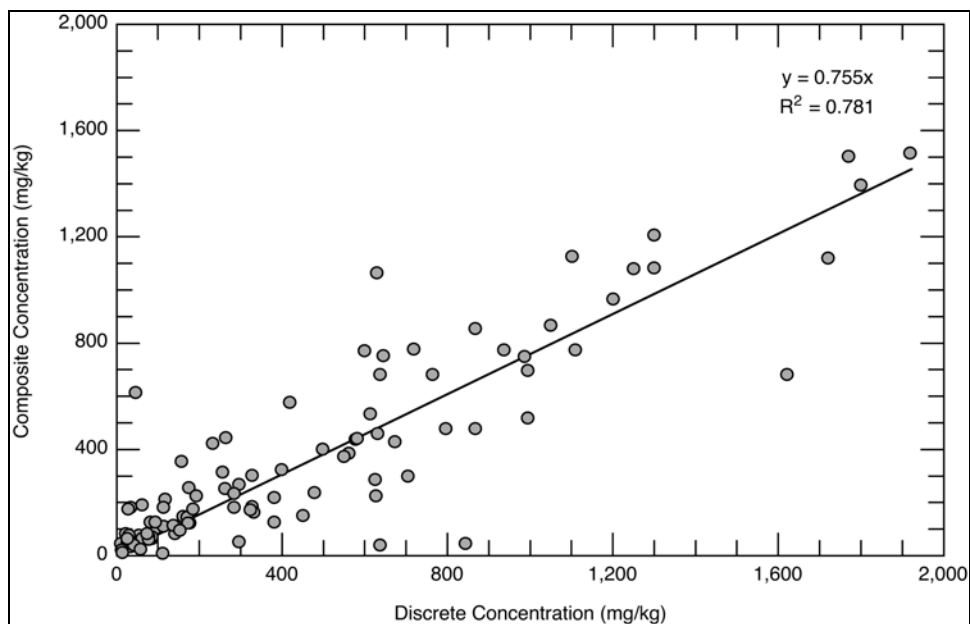


Figure 29. Comparison of HMX concentration in discrete and composite soil samples collected in Grid 10.

As indicated above for the grid samples, HMX was present at concentrations two orders of magnitude above any other analyte with a maximum concentration of 1,230 mg/kg. A plot of the concentrations of HMX as a function of sampling position is shown in Figure 30. The mean concentration for HMX for the four halo samples closest to the central target was 898 mg/kg with decreasing concentrations in the two outer halos of 199 and 113 mg/kg, respectively. The concentrations in the outer halo appear to be influenced by the presence of two other targets located in these zones. Otherwise an even greater decrease in concentration within this outer halo would have been observed as can be seen for the segments farthest from the targets (Fig. 30). The same type of concentration decrease relative to distance from the central target was observed for RDX, TNT, 4ADNT, and 2ADNT, but not for NG. The reason for this is that the NG originates from the propellant used in these rockets while the other analytes, like HMX, are associated with the high explosive. Rockets are propelled all the way to the target and hence the deposition occurs as the rocket flies overhead. The concentration pattern for NG relative to sample position is shown in Figure 31. Note that the concentration in this figure is in $\mu\text{g}/\text{kg}$ rather than mg/kg , which is used for HMX in Figure 30. The three highest NG concentrations are in segments nearest to the three targets, but otherwise, the distribution of NG in the target area appears more random than that for HMX.

Table 10. Analytical results from RP-HPLC analysis of composite soil samples collected in halo sections around target at various distances.							
Sample	Soil concentrations (mg/kg)						
Field #	HMX	RDX	TNT	NG	2,4-DNT	2ADNT	4ADNT
5 m around tank target							
A1 AT	1230	5.20	8.22	7.56	<d	3.38	3.68
A2 AT	1100	5.38	6.96	17.0	<d	2.46	2.62
A3 AT	924	0.380	8.58	3.48	<d	1.50	1.48
A4 AT	336	<d	3.52	2.98	<d	0.72	0.66
15 m around tank target							
B1 AT	106	<d	0.050	0.080	<d	0.120	0.112
B2 AT	236	0.120	1.48	0.482	<d	0.266	0.258
B3 AT	140	0.076	0.360	0.130	<d	0.238	0.236
B4 AT	100	0.168	0.126	0.616	<d	0.110	<d
B5 AT	154	0.234	1.63	1.34	<d	0.220	0.198
B6 AT	310	0.064	4.84	1.35	0.090	0.460	0.410
B7 AT	390	0.476	1.79	1.62	0.340	0.836	0.746
B8 AT	157	0.074	3.00	0.626	<d	0.290	0.274
25 m around tank target							
C1 AT	21.8	<d	0.440	0.662	<d	<d	<d
C2 AT	35.8	<d	<d	0.204	<d	<d	<d
C3 AT	42.2	<d	<d	0.320	<d	<d	<d
C4 AT	9.84	<d	<d	0.830	<d	<d	<d
C5 AT	49.4	0.054	1.00	1.03	<d	<d	<d
C6 AT	14.1	<d	<d	<d	0.310	<d	<d
C7 AT	14.3	<d	0.120	<d	<d	<d	<d
C8 AT	91.6	0.102	6.76	2.22	<d	0.146	0.154
C9 AT	125	0.338	3.08	0.852	<d	0.268	0.288
C10 AT	183	0.170	0.918	8.46	<d	0.264	0.304
C11 AT	188	<d	0.848	0.436	<d	0.208	0.178
C12 AT	230	0.056	5.36	0.380	<d	0.214	0.202
C13 AT	238	0.714	6.34	0.560	0.328	0.248	0.234
C14 AT	250	0.346	1.72	6.74	0.062	0.816	0.804
C15 AT	262	0.228	4.48	23.4	0.352	0.720	0.750
C16 AT	44.6	<d	0.128	1.25	<d	0.110	0.104

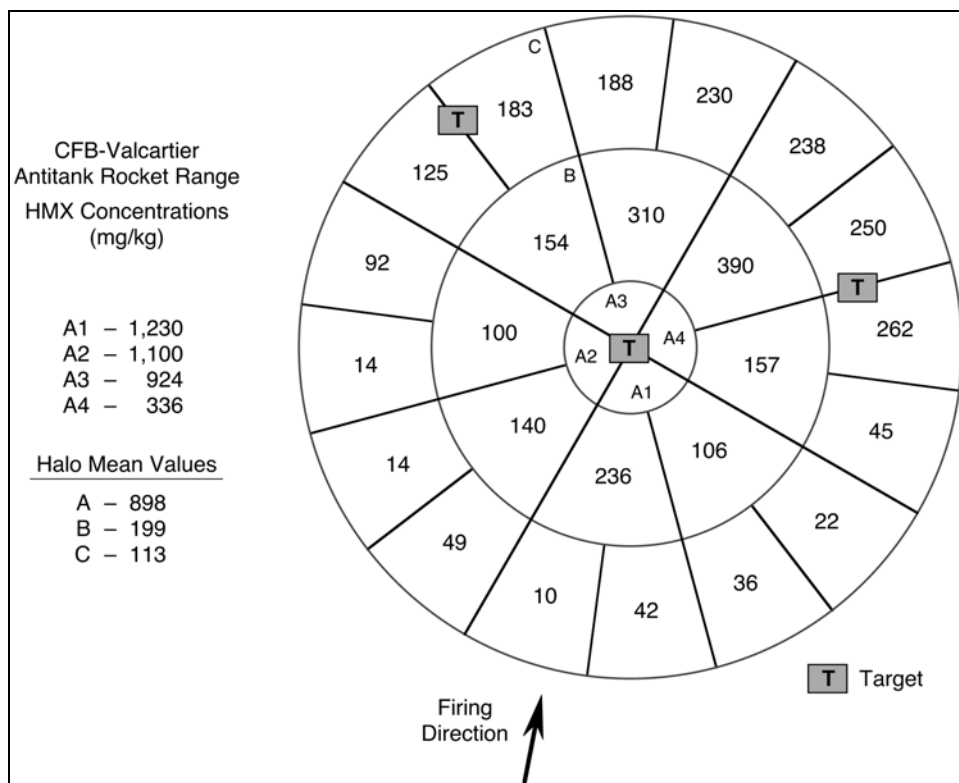


Figure 30. Concentration of HMX relative to sample position around target.

These results confirm earlier results that lead to a recommended sampling strategy using a concentric ring pattern (Jenkins et al. 1998). That pattern is similar to the strategy employed here except that the halos are not subdivided and samples are collected within smaller intervals from the target. The pattern employed here provides more information about the radial distribution of the contamination, whereas using concentric ring strategy (Fig. 2) with the same number of total samples provides more information on the concentration as a function of distance from the target.

Water Sample Results

Only one water sample was collected from the small stream that runs across the antitank firing range at CFB-Valcartier (Fig. 6). Upon analysis, the concentrations of HMX, RDX, and TNT were 129, 2.4, and 1.6 $\mu\text{g/L}$, respectively. These concentrations were surprisingly high although the total flow rate of the stream was very small on the day that we sampled. The weather conditions at the time of sampling were cloudy, cool, and light mist.

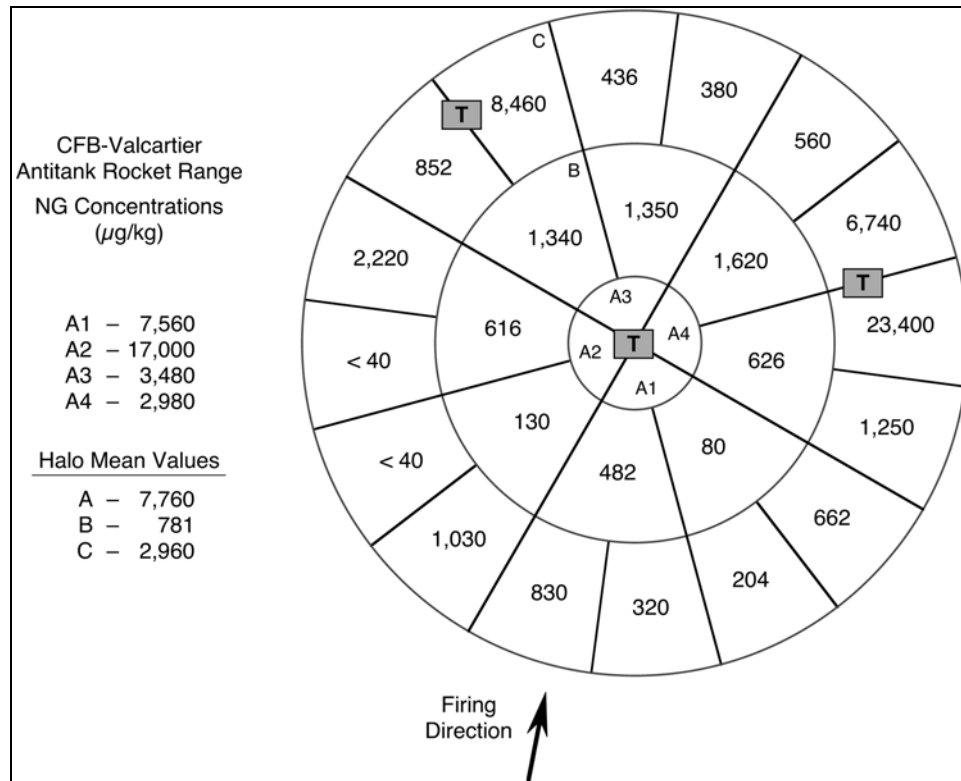


Figure 31. Concentration of NG relative to sample position around targets.

Assessment of Subsampling Error for Composite Soil Samples

From past work we have determined that subsampling error can be important when attempting to obtain a representative portion of a large sample for extraction and analysis. This is of particular concern when the field sample is a large multi-increment composite. In an attempt to minimize the subsampling contribution to the total characterization uncertainty, we have developed a procedure that utilizes a puck-mill grinder to reduce the particle size of the material before mixing and subsampling. The exact procedure that we used for these samples is provided above.

To evaluate the subsampling uncertainty, 24 composite samples were selected for additional attention. For each of these samples two additional subsamples were obtained and processed in an identical manner to the routine subsample for all composites. Thus, for these 24 samples, three subsamples of each were extracted and analyzed using RP-HPLC-UV (Table 11).

There were seven target analytes detected in these samples. NG was detected in all three replicates of 18 of these samples. In each case the % relative standard deviation was computed and these values were averaged to provide a mean % relative standard deviation. For NG this value was 46.5%. Similar calculations were performed for HMX, RDX, TNT, 2ADNT, and 4ADNT and the pooled relative standard deviations were 5.0%, 6.6%, 13.6%, 10.5%, and 8.1%, respectively (Table 12). There was insufficient data for 2,4-DNT. Clearly the mean % relative standard deviation for NG is much higher than for the other analytes. This result confirms the findings of Walsh et al. (2004) and Hewitt and Walsh (2003) who found that it was much more difficult to obtain consistent subsamples for compounds deposited from propellants than for explosives. As stated above, NG is deposited at this range from propellant particles, whereas the other analytes originate from the high explosive in the warhead of the LAW rocket. The puck-mill grinder is apparently less effective at reducing the particle size of propellants than crystalline high explosives.

Table 11. Analytical results for replicate subsamples of selected composite samples (analysis by RP-HPLC).

Field #	Soil concentrations, mg/kg						
	HMX	RDX	TNT	NG	2,4-DNT	2ADNT	4ADNT
G10	410	0.690	5.02	0.566	<d	0.984	1.014
G10 LD1	382	0.632	4.68	0.446	<d	0.904	0.948
G10 LD2	404	0.610	4.98	0.830	<d	0.992	1.016
B3 AT	140	0.076	0.360	0.130	<d	0.238	0.236
B3 AT LD1	157	0.082	0.538	1.21	<d	0.280	0.246
B3 AT LD2	146	0.084	0.342	0.374	<d	0.278	0.266
C4 AT	9.84	<d	<d	0.830	<d	<d	<d
C4 AT LD1	9.70	<d	<d	0.926	<d	<d	<d
C4 AT LD2	10.08	<d	<d	0.610	<d	<d	<d
C13 AT	238	0.714	6.34	0.560	0.328	0.248	0.234
C13 AT LD1	222	0.642	5.96	0.076	<d	0.220	0.214
C13 AT LD2	254	0.774	6.84	0.562	0.082	0.308	0.282
G3-C7	<d	<d	<d	0.246	<d	<d	<d
G3-C7 LD1	<d	<d	<d	0.172	<d	<d	<d
G3-C7 LD2	<d	<d	<d	0.084	<d	<d	<d
G3-C17	<d	<d	0.004	0.156	<d	<d	<d
G3-17 LD1	<d	<d	0.002	0.188	<d	<d	<d
G3-17 LD2	<d	<d	0.004	0.176	<d	<d	<d

Table 11 (cont'd). Analytical results for replicate subsamples of selected composite samples (analysis by RP-HPLC).

Field #	Soil concentrations, mg/kg						
	HMX	RDX	TNT	NG	2,4-DNT	2ADNT	4ADNT
G10-C37	44.4	0.360	0.540	<d	<d	<d	<d
G10-C37 LD1	45.2	0.380	0.460	<d	<d	<d	<d
G10-C37 LD2	48.4	0.402	0.606	<d	<d	0.500	0.680
G10-C47	402	0.260	2.66	3.32	<d	0.500	0.360
G10-C47 LD1	360	<d	2.08	1.28	<d	<d	<d
G10-C47 LD2	368	<d	2.28	3.44	1.28	<d	<d
G10-C57	322	<d	0.940	5.02	<d	<d	<d
G10-C57 LD1	330	<d	0.960	8.06	<d	<d	<d
G10-C57 LD2	312	<d	0.680	7.84	<d	<d	<d
G10-C67	234	<d	<d	6.28	<d	<d	<d
G10-C67 LD1	230	<d	<d	3.34	<d	<d	<d
G10-C67 LD2	234	<d	<d	2.52	<d	<d	<d
G10-C77	150	<d	0.420	3.24	<d	<d	<d
G10-C77 LD1	160	<d	0.400	4.88	<d	<d	<d
G10-C77 LD2	159	<d	<d	<d	<d	<d	<d
G10-C87	40.2	<d	<d	0.092	<d	<d	<d
G10-C87 LD1	44.8	<d	<d	<d	<d	<d	<d
G10-C87 LD2	45.0	<d	<d	<d	<d	<d	<d
G10-C97	60.4	<d	1.29	0.086	<d	0.112	0.106
G10-C97 LD1	69.8	<d	1.38	0.042	<d	0.132	0.12
G10-C97 LD2	67.2	<d	1.38	0.322	<d	<d	<d

Table 12. Mean % relative standard deviation for laboratory duplicates.

Target analyte	n	Mean % RSD
NG	18	46.5
HMX	12	5.0
RDX	4	6.6
TNT	10	13.6
2ADNT	3	10.5
4ADNT	3	8.1

5 SUMMARY AND RECOMMENDATIONS

Major Residues and Locations on Antitank Rocket Ranges

Results from this and other characterization studies provide information that can be used to stratify the various areas of antitank ranges with respect to the major residues present as a function of location. The major munition fired at these ranges is the M72 66-mm LAW rocket. This weapon has a warhead that contains octol that is composed of 70/30 HMX/TNT. The propellant used in this weapon is double-based, composed of 70/30 NC/NG. Because these rockets are propelled all the way to the targets, NG is detectable at most locations on the range, and in particular, behind the firing line. NC is undoubtedly present as well, but because it is a polymer and insoluble in water, it is not a concern for off-site migration. Concentrations of NG between the firing line and the target are generally in the low ppm range or below, but they can be orders of magnitude higher for distances of at least 50 m behind the firing line due to the back blast of this weapon. Chunks of propellant can also be found at the target because these thin-walled munitions sometimes shear open upon impact without detonating, releasing residual propellant as particulates of various sizes.

At the target, HMX is the major residue present with concentrations generally two orders of magnitude higher than TNT. There is a strong concentration gradient present near the target and the highest concentrations are generally in front of the targets where deposition occurs mainly from ruptured rockets that did not detonate upon impact. Concentrations of HMX as high as the thousands of mg/kg have been found in surface soils at antitank rocket ranges, but the concentrations decline rapidly with depth below the first few centimeters.

Sampling Strategy for Characterization at Antitank Rocket Ranges

Based on the results from this work, we recommend that sampling at antitank ranges be conducted as follows. Within the impact area, the surface soils in the area around the targets should be sampled using either the segmented halo approach developed by Ampleman et al. (2003a, b) and shown in Figures 30 and 31, or the concentric ring sampling approach recommended by Jenkins et al. (1997), as shown in Figure 2. The choice should depend on whether the directionality of the concentrations are of major importance to characterize or not. In either case, duplicate samples should be collected as often as feasible to allow an estimate of uncertainty in the concentrations obtained.

HMX will be the contaminant present at highest concentration and the concentrations will vary from range to range depending upon the usage. A concentration gradient will be present and will be captured using either approach. The depth of sampling for the surface soils should be 0 to 2.5 cm since the contamination occurs from deposition of particles mainly from the rupture of undetonated rockets and from rockets that undergo partial detonations. Shallow subsurface samples should also be taken near the targets to determine the concentration gradient with depth. Collection of these samples may be limited, however, for safety reasons.

Near the firing point, the major contaminant is NG, which is much higher in concentration behind the firing line than between the firing line and the targets. Surface soils (0 to 2.5 cm) in the area behind the firing line should be sampled using area composites at 5-m intervals. The area between the firing line and the target could also be sampled using square grids as conducted here.

All samples used to estimate the mean concentration for given areas of the range should be multi-increment composite samples. We recommend that at least 30 increments be used per composite based on the tolerance ranges estimated here (Table 5). The uncertainty associated with discrete samples or multi-increment composite samples with small values of n may often be unacceptable (Table 5).

Soil Subsampling

Subsampling error can be large if samples are not properly processed to control distributional and compositional heterogeneity prior to subsampling. This is particularly true for large composite samples that are often a kilogram in mass and where only a 10-g portion is extracted and analyzed.

There appears to be a difference in the ability to adequately process soils containing residues of explosives and residues of propellant prior to subsampling. For example, the analytical results for HMX, TNT, and RDX from replicate subsamples of soil in this study showed a mean pooled % relative standard deviation of about 54% (Table 12). The pooled % relative standard deviation for NG, however, was 250%, demonstrating a much poorer ability to adequately process soils containing residues of this compound prior to subsampling. We speculate that this difference is due to a difference in the physical characteristics of explosives and propellant residues (Walsh et al. 2004). Research to address this issue is underway.*

* Personal communication, M.E. Walsh, ERDC-CRREL, 2004.

At present we recommend the following procedure. Spread the soil sample on a clean surface and air-dry. Break up clumps of soil in a mortar and pestle and sieve through a 10-mesh (2.0-mm) sieve. The mesh size is a deviation from that specified in Method 8330 (Hewitt et al. in press). Grind the entire sample with a mechanical grinder to reduce the particle size to a fine flour. Spread the ground material in a thin layer on a clean surface and build a subsample of 10 g by taking multiple increments of soil from random locations. Collect sufficient replicates to verify that subsampling error has been reduced to acceptable levels.

Chemical Analysis of Soil Extracts

The most important target analytes for characterization of soils samples from antitank rocket ranges are HMX and NG, followed by RDX, TNT, 2ADNT, and 4ADNT. SW846 Method 8330 (EPA 1994) is an RP-HPLC-UV method that targets 14 energetic analytes, including HMX, RDX, TNT, 2ADNT, and 4ADNT. Unfortunately, NG is not a target analyte for Method 8330. Within our laboratory and at some contract laboratories, Method 8330 has been modified by using either a dual UV detector (210 nm and 254 nm) or a diode array detector on the HPLC instrument instead of a single detector set to 254 nm. If this is done, NG can be determined using the same analytical protocol as used for the 14 standard analytes. When NG or PETN are detected, however, they must be confirmed using a second column or by GC-ECD because there are many more potential interferences that absorb at the 210-nm wavelength than at the 254-nm wavelength used for the normal target analyte list.

The detection limits for Method 8330 in our laboratory are provided in Table 1. For the major analytes at antitank ranges, our detection limits are all below 38 $\mu\text{g}/\text{kg}$. For most applications, we believe these detection limits are adequate.

Another option for analysis of soil extracts for these compounds is SW846 Method 8095 (EPA 1999). The detection limits for Method 8095 in our laboratory are also given in Table 1. For most of the analytes, these detection limits are about an order of magnitude lower than achievable using Method 8330. For some studies this difference may be useful. The detection limits for HMX, however, are equivalent for both methods. Also, the low volatility and high thermal lability of HMX has proved to be troublesome for GC- and GC/MS-based methods.

REFERENCES

Ampleman, G., S. Thiboutot, J. Lewis, A. Marois, A. Gagnon, M. Bouchard, R. Martel, R. Lefebvre, T.A. Ranney, T.F. Jenkins, and J.C. Pennington (2003a) Evaluation of the impacts of live-fire training at CFB Shilo (final report). Defence Research Development Canada–Valcartier, Technical Report TR 2003-066, April 2003.

Ampleman, G., S. Thiboutot, J. Lewis, A. Marois, A. Gagnon, M. Bouchard, S. Jean, T. Jenkins, A. Hewitt, J.C. Pennington, and T.A. Ranney (2003b) Evaluation of the contamination by explosives at Cold Lake Air Weapons Range (CLAWR), Alberta: Phase 1 Report. Defence Research Development Canada–Valcartier, Technical Report TR 2003-208, December 2003.

Environmental Protection Agency (1994) Nitroaromatics and nitramines by HPLC. Second Update SW846 Method 8330.

Environmental Protection Agency (1999) Nitroaromatics and nitramines by GC-ECD. Fourth Update SW846 Method 8095.

Grant, C.L., T.F. Jenkins, and S.M Golden (1993) Experimental assessment of analytical holding times for nitroaromatic and nitramine explosives in soil. U.S. Army Cold Regions Research and Engineering Laboratory, Hanover, New Hampshire, Special Report 93-11.

Hewitt, A.D., and M.E. Walsh (2003) On-site processing and subsampling of surface soils samples for the analysis of explosives. U.S. Army Engineer Research and Development Center, Hanover, New Hampshire, Technical Report ERDC/CRREL TR-03-14.

Hewitt, A.D., T.F. Jenkins, T.A. Ranney, D. Lambert, and N. Perron (in press) Characterization of energetic residues at military firing ranges: Schofield Barracks and Pohakuloa Training Area. Engineer Research and Development Center Technical Report.

Jenkins, T.F., C.L. Grant, G.S. Brar, P.G. Thorne, T.A. Ranney, and P.W. Schumacher (1996) Assessment of sampling error associated with collection and analysis of soil samples at explosives contaminated sites. U.S. Army Cold Regions Research and Engineering Laboratory, Hanover, New Hampshire, Special Report 96-15.

Jenkins, T.F., M.E. Walsh, P.G. Thorne, S. Thiboutot, G. Ampleman, T.A. Ranney, and C.L. Grant (1997) Assessment of sampling error associated with the collection and analysis of soil samples at a firing range contaminated with HMX. U.S. Army Cold Regions Research and Engineering Laboratory, Hanover, New Hampshire, Special Report 97-22.

Jenkins, T.F., M.E. Walsh, P.G. Thorne, P.H. Miyares, T.A. Ranney, C.L. Grant, and J. Esparza (1998) Site characterization for explosives at a military firing range impact area. U.S. Army Cold Regions Research and Engineering Laboratory, Hanover, New Hampshire, Special Report 98-9.

Jenkins, T.F., C.L. Grant, M.E. Walsh, P.G. Thorne, S. Thiboutot, G. Ampleman, and T.A. Ranney (1999) Coping with spatial heterogeneity effects on sampling and analysis at an HMX-contaminated antitank firing range. *Field Analytical Chemistry and Technology*, **3**(1): 19–28.

Lynch, J.C., J.M. Brannon, and J.J. Delfino (2002) Dissolution rates of three high explosive compounds: TNT, RDX, and HMX. *Chemosphere*, **47**: 725–734.

Natrella, M.G. (1963) Experimental Statistics, National Bureau of Standards Handbook 91. Washington, D.C.: U.S. Government Printing Office.

Pennington, J.C., T.F. Jenkins, G. Ampleman, S. Thiboutot, J.M. Brannon, J. Lynch, T.A. Ranney, J. Stark, M.E. Walsh, J. Lewis, C.A. Hayes, J.E. Mirecki, A.D. Hewitt, N. Perron, D. Lambert, J. Clausen, and J.J. Delfino (2002) Distribution and fate of energetics on DoD test and training ranges: Interim Report 2. U.S. Army Engineer Research and Development Center, Environmental Laboratory, Vicksburg, Mississippi, ERDC Technical Report TR-02-8.

Pennington, J.C., T.F. Jenkins, G. Ampleman, S. Thiboutot, J.M. Brannon, J. Lewis, J.E. DeLaney, J. Clausen, A.D. Hewitt, M.A. Hollander, C.A. Hayes, J.A. Stark, A. Marois, S. Brochu, H.Q. Dinh, D. Lambert, A. Gagnon, M. Bouchard, R. Martel, P. Brousseau, N.M. Perron, R. Lefebvre, W. Davis, T.A. Ranney, C. Gauthier, S. Taylor, and J. Ballard (2003) Distribution and fate of energetics on DoD test and training ranges: Interim Report 3. U.S. Army Engineer Research and Development Center, Environmental Laboratory, Vicksburg, Mississippi, ERDC Technical Report TR-03-2.

Price, C.B., J.M. Brannon, and C. Hayes (1997) Transformation of RDX and HMX under controlled Eh/pH conditions. U.S. Army Engineer Waterways Experiment Station, Vicksburg, Mississippi, Technical Report IRRP-98-2.

Thiboutot, S., G. Ampleman, A. Gagnon, A. Marois, T.F. Jenkins, M.E. Walsh, P.G. Thorne, and T.A. Ranney (1998) Characterization of antitank firing ranges at CFB Valcartier, WATC Wainwright, and CFAD Dundurn. Defence Research Establishment Valcartier, Quebec, Report # DREV-R-9809.

Thiboutot, S., G. Ampleman, J. Lewis, D. Faucher, A. Marois, R. Martel, J.M. Ballard, S. Downe, T. Jenkins, and A. Hewitt (2003) Environmental conditions of surface soils and biomas prevailing in the training area at CFB Gagetown, New Brunswick. Defence Research and Development Canada Valcartier, Technical Report TR-2003-152.

Walsh, M.E., C.M. Collins, C.H. Racine, T.F. Jenkins, A.B. Gelvin, and T.A. Ranney (2001) Sampling for explosives residues at Fort Greely, Alaska: Reconnaissance visit July 2000. U.S. Army Engineer Research and Development Center, Hanover, New Hampshire, Technical Report ERDC/CRREL TR-01-15.

Walsh, M.E., C.M. Collins, A.D. Hewitt, M.R. Walsh, T.F. Jenkins, J. Stark, A. Gelvin, T. Douglas, N. Perron, D. Lambert, R. Bailey, and K. Myers (2004) Range characterization studies at Donnelly Training Area, Alaska 2001 and 2002. U.S. Army Engineer Research and Development Center, Hanover, New Hampshire, Technical Report ERDC/CRREL TR-04-3.

REPORT DOCUMENTATION PAGE

Form Approved
OMB No. 0704-0188

Public reporting burden for this collection of information is estimated to average 1 hour per response, including the time for reviewing instructions, searching existing data sources, gathering and maintaining the data needed, and completing and reviewing this collection of information. Send comments regarding this burden estimate or any other aspect of this collection of information, including suggestions for reducing this burden to Department of Defense, Washington Headquarters Services, Directorate for Information Operations and Reports (0704-0188), 1215 Jefferson Davis Highway, Suite 1204, Arlington, VA 22202-4302. Respondents should be aware that notwithstanding any other provision of law, no person shall be subject to any penalty for failing to comply with a collection of information if it does not display a currently valid OMB control number. PLEASE DO NOT RETURN YOUR FORM TO THE ABOVE ADDRESS.

1. REPORT DATE (DD-MM-YY) April 2004		2. REPORT TYPE Technical Report		3. DATES COVERED (From - To)		
4. TITLE AND SUBTITLE Representative Sampling for Energetic Compounds at an Antitank Firing Range				5a. CONTRACT NUMBER		
				5b. GRANT NUMBER		
				5c. PROGRAM ELEMENT NUMBER		
6. AUTHOR(S) Thomas F. Jenkins, Thomas A. Ranney, Alan D. Hewitt, Marianne E. Walsh, and Kevin L. Bjella				5d. PROJECT NUMBER		
				5e. TASK NUMBER		
				5f. WORK UNIT NUMBER		
7. PERFORMING ORGANIZATION NAME(S) AND ADDRESS(ES) U.S. Army Engineer Research and Development Center Cold Regions Research and Engineering Laboratory 72 Lyme Road Hanover, NH 03755-1290				8. PERFORMING ORGANIZATION REPORT ERDC/CRREL TR-04-7		
9. SPONSORING/MONITORING AGENCY NAME(S) AND ADDRESS(ES)				10. SPONSOR / MONITOR'S ACRONYM(S)		
				11. SPONSOR / MONITOR'S REPORT NUMBER(S)		
12. DISTRIBUTION / AVAILABILITY STATEMENT Approved for public release; distribution is unlimited. Available from NTIS, Springfield, Virginia 22161.						
13. SUPPLEMENTARY NOTES						
14. ABSTRACT Field sampling experiments were conducted at the CFB-Valcartier Arnhem antitank rocket range to investigate various sampling schemes that would yield representative soil samples at firing points and impact areas of antitank ranges. Three sampling strategies were evaluated. Between the firing point and the target, 10-m x 10-m grids were established and 30-increment composite soil samples were collected. In two of these grids, one near the firing point and one at the target, the grids were divided into 100 1-m x 1-m minigrids. Within each minigrid a discrete and a 10-increment composite soil sample were collected and analyzed for energetic compounds. In the target area, an alternative strategy was also evaluated using concentric halos around the target. Each halo was subdivided into increasing numbers of segments at increasing distances from the targets. Multi-increment composite samples were collected within each halo segment. Behind the firing line, nine line (linear) composites were collected at various distances from 0 to 25 m from the firing line. Results from the 100 1-m x 1-m minigrids near the firing line and the target demonstrated that the distribution of analyte concentrations in the discrete samples was non-Gaussian and the range of concentrations varied over two orders of magnitude. The distributions of data for multi-increment composite samples with various numbers of increments were simulated by averaging the concentration estimates from randomly selected discrete samples. For the firing line area, the distribution of NG computed composites exhibits increased normality as the number of increments is increased and the resulting tolerance range declined substantially. This was also true for HMX in the target area. Recommendations are made for appropriate sampling strategies to collect representative surface soil samples for antitank rocket ranges.						
15. SUBJECT TERMS						
Antitank range		Explosives residues		Propellants		
Composite sampling		HMX		Representative sampling		
Explosives		NG		Site characterization		
16. SECURITY CLASSIFICATION OF:				17. LIMITATION OF OF ABSTRACT	18. NUMBER OF PAGES	19a. NAME OF RESPONSIBLE PERSON
a. REPORT	b. ABSTRACT	c. THIS PAGE	19b. TELEPHONE NUMBER (include area code)			
U	U	U	U	72		